



Holocene land cover change in North America: continental 2 trends, regional drivers, and implications for vegetation- atmosphere feedbacks

4

Andria Dawson*^{†1}, John W. Williams^{†2}, Marie-José Gaillard³, Simon J Goring², Behnaz
6 Pirzamanbein⁴, Johan Lindstrom⁵, R. Scott Anderson⁶, Andrea Brunelle⁷, David Foster⁸, Konrad
Gajewski⁹, Daniel G. Gavin¹⁰, Terri Lacourse¹¹, Thomas A Minckley¹², Wyatt Oswald¹³, Bryan
8 Shuman¹², Cathy Whitlock¹⁴

10 ¹Department of Mathematics and Computing, Department of Biology, Mount Royal University, Calgary, AB
T3E6K6

12 ²Department of Geography and Center for Climatic Research, University of Wisconsin-Madison, Madison, WI
53706

14 ³Department of Biology and Environmental Science, Linnaeus University, SE 39231 Kalmar, Sweden

⁴Department of Statistics, School of Economics and Management, Lund University, SE-220 07 Lund, Sweden

16 ⁵Division of Mathematical Statistics, Centre for Mathematical Sciences, Lund University, SE-221 00 Lund, Sweden

⁶School of Earth and Sustainability, Northern Arizona University, Flagstaff, AZ 86011

18 ⁷Geography Department, University of Utah, Salt Lake City, UT 84112

⁸Harvard Forest, Harvard University, Petersham, MA 01366

20 ⁹Département de Géographie, Environnement et Géomatique, Université d'Ottawa, Ottawa, ON K1N 6N50

¹⁰Department of Geography, University of Oregon, Eugene, OR 97403

22 ¹¹Department of Biology and Centre for Forest Biology, University of Victoria, Victoria, BC V8P 5C2

¹²Department of Geology and Geophysics, University of Wyoming, Laramie, WY 82071

24 ¹³Marlboro Institute for Liberal Arts and Interdisciplinary Studies, Emerson College, Boston, MA 02116 and

¹⁴Department of Earth Sciences, Montana State University, Bozeman, MT 59717

26

*Correspondence email: adawson@mtroyal.ca

28 [†]These authors contributed equally to the development of this manuscript



30 Abstract

32 Land cover governs the biogeophysical and biogeochemical feedbacks between the land surface and
33 atmosphere. Holocene vegetation-atmosphere interactions are of particular interest, both to understand the
34 climate effects of intensifying human land use and as a possible explanation for the Holocene
35 Conundrum, a widely studied mismatch between simulated and reconstructed temperatures. Progress has
36 been limited by a lack of data-constrained, quantified, and consistently produced reconstructions of
37 Holocene land cover change. As a contribution to the Past Global Changes (PAGES) LandCover6k
38 Working Group, we present a new suite of land cover reconstructions with uncertainty for North America,
39 based on a network of 1445 sedimentary pollen records and the REVEALS pollen-vegetation model
40 coupled with a Bayesian spatial model. These spatially comprehensive land cover maps are then used to
41 determine the pattern and magnitude of North American land cover changes at continental to regional
42 scales. Early Holocene afforestation in North America was driven by rising temperatures and
43 deglaciation, and this afforestation likely amplified early Holocene warming via the albedo effect. A
44 continental-scale mid-Holocene peak in summergreen trees and shrubs (8.5 to 4 ka) is hypothesized to
45 represent a positive and understudied feedback loop among insolation, temperature, and phenology
46 seasonality. A last-millennium decrease in summergreen trees and shrubs with corresponding increases in
47 open land likely was driven by a spatially varying combination of intensifying land use and neoglacial
48 cooling. Land cover trends vary within and across regions, due to individualistic taxon-level responses to
49 environmental change. Major species-level events, such as the mid-Holocene decline of eastern hemlock,
50 may have altered regional climates. The substantial land-cover changes reconstructed here support the
51 importance of biogeophysical vegetation feedbacks to Holocene climate dynamics. However, recent
52 model experiments that invoke vegetation feedbacks to explain the Holocene Conundrum may have
53 overestimated the land cover forcing by replacing Northern Hemisphere grasslands >30°N with forests;
54 an ecosystem state that is not supported by these land cover reconstructions. These Holocene
55 reconstructions for North America, along with similar LandCover6k products now available for other
56 continents, serve the Earth system modeling community by providing better-constrained land cover
57 scenarios and benchmarks for model evaluation, ultimately making it possible to better understand the
58 regional- to global-scale processes driving Holocene land cover dynamics.

58



1. Introduction

60 Vegetation is the great mediator of biogeophysical and biogeochemical interactions between the land
62 surface and the atmosphere (Bonan and Doney, 2018; Harrison et al., 2020; Pongratz et al., 2010; Gaillard
64 et al., 2010). Enhanced carbon uptake and sequestration by terrestrial ecosystems is an essential
66 component to contemporary negative-net CO₂ emission scenarios needed to stabilize the climate system
68 and mitigate the dangerous impacts already emerging (Rogelj et al., 2018; van Vuuren et al., 2017).
During the Holocene, as cryosphere-ocean-atmosphere feedbacks waned and anthropogenic land use
66 intensified (Ruddiman, 2013; Stephens et al., 2019), vegetation-atmosphere feedbacks and forcings
68 increased in importance, particularly in regions where climate variability interacted with major changes in
68 vegetation structure. Examples include soil and vegetation feedbacks that amplified precessional-driven
70 variations in monsoonal rainfall intensity in North Africa and Asia (Chen et al., 2021; Chandan and
70 Peltier, 2020), and increases in high-latitude tree cover, which decreased wintertime albedo and increased
72 temperatures (Williams et al., 2011; TEMPO (Testing Earth System Models with Paleo-Observations),
72 1996; Foley et al., 1994). Intensified human land use and resulting greenhouse gas emissions may have
74 delayed Northern Hemisphere late-Holocene cooling and glaciation (Ruddiman, 2003). However, initial
74 models of global anthropogenic land cover change (ALCC) (Kaplan et al., 2009; Klein Goldewijk et al.,
76 2011, 2010) over the Holocene were largely unconstrained by paleoecological and archaeological
76 observations and so differed widely in their estimated size and scope of the anthropogenic footprint. More
78 recently, Holocene increases in vegetation cover have been invoked to explain the Holocene Temperature
78 Conundrum, a discrepancy between proxy and model-estimated temperature during the early- to mid-
80 Holocene (Thompson et al., 2022; Kaufman and Broadman, 2023), but global simulations of vegetation-
80 climate feedbacks during the Holocene are not constrained by observational data. At subcontinental
82 scales, data-constrained studies of Holocene climate-vegetation feedbacks in Europe indicate that mid-
82 Holocene vegetation changes relative to pre-Industrial baselines could have warmed winters in some
areas by 4-6°C in northeastern Europe (Strandberg et al., 2022a, 2014).

84 Hence, there is an on-going need for comprehensive and accurate proxy-based reconstructions of
past land cover at regional to global extents (Gaillard and Group, 2015; Gaillard et al., 2018, 2010). These
86 reconstructions can then be used with Earth system models (ESMs) to test hypotheses about the physical,
biological, and anthropogenic processes that drove Holocene climate variability (Harrison et al., 2020).
88 Fossil pollen records offer the primary observational constraint on past vegetation composition and
structure, with thousands of records now available globally. Efforts to systematically map late-Quaternary
90 land cover using fossil pollen data and well-defined rulesets began in the late 1990s with the Biome6000
project (Prentice et al., 2000, 2011). Since then, the continental-scale pollen databases launched in the



92 1980s and 1990s (Grimm et al., 2013) have coalesced along with other paleoecological data into the
Neotoma Paleocology Database (Neotoma), an international, multi-proxy, curated data resource that
94 helps tame issues of data heterogeneity through community curation by experts (Williams et al., 2018).
Neotoma thus enables global-scale analyses of past vegetation and climate change (e.g. Mottl et al., 2021;
96 Herzs Schuh et al., 2023).

Multiple pollen-vegetation models (PVMs) have been developed to make quantitative inferences
98 about past vegetation. Some PVMs involve relatively simple but effective transfer functions, such as the
modern analogue technique (Williams et al., 2011) or rule-based systems for classifying land cover
100 (Prentice et al., 2000; Cruz-Silva et al., 2022; Fyfe et al., 2010). Others are process-based proxy system
models (Evans et al., 2013) that attempt to represent the processes governing the atmospheric transport
102 and deposition of pollen, such as the REVEALS and LOVE (Sugita, 2007a, c) or STEPPS (Dawson et al.,
2019a). Efforts continue to test and refine the parameterizations of these models through paired analyses
104 of pollen assemblages and forest composition at local to landscape scales (Liu et al., 2022).

In response to these scientific needs and opportunities, the Past Global Changes (PAGES)
106 LandCover6k working group was launched as an international effort (Gaillard and Group, 2015) to
reconstruct vegetation globally for the Holocene. LandCover6k, led by experts typically working at
108 continental scales, has had the explicit aim of creating vegetation reconstructions that can better constrain
past histories of anthropogenic land use in ESMs and is mostly based on networks of fossil pollen
110 records. To facilitate the use of these vegetation reconstructions in ESMs, the REVEALS PVM has been
used for all LandCover6k reconstructions, with standard model parameterizations and standard protocols
112 for pollen data handling. LandCover6k gridded REVEALS reconstructions at the continental scale have
been published so far for Europe (Githumbi et al., 2022a, b; Trondman et al., 2015; Serge et al., 2023) and
114 China (Li et al., 2023b). However, no comparable REVEALS-based land cover reconstructions are
available for North America, despite a comparable density of fossil pollen records to these other regions
116 (Stegner and Spanbauer, 2023) and prior regional-scale applications of REVEALS in North America
(Sugita et al., 2010; Chaput and Gajewski, 2018).

118 REVEALS uses pollen counts, pollen productivity estimates, pollen fall speeds, atmospheric
conditions, and sedimentary basin type and size to estimate vegetation composition for a given time
120 period. REVEALS accounts for the processes of differential pollen production (determined by pollen
productivity estimates) and dispersal-deposition (determined by the pollen fall speeds, atmospheric
122 conditions, and sedimentary basin type and size).

While REVEALS reconstructions usually combine information from multiple pollen records, REVEALS
124 is not explicitly spatial, and so does not support the interpolation of inferences to places with no pollen
records. To address this issue, other researchers have developed a statistical approach to spatially



126 interpolate REVEALS-based land cover estimates from individual grid cells to all cells within the grid,
including estimates of uncertainty (Pirzamanbein et al., 2014, 2018a). The approach uses a Bayesian
128 hierarchical model with spatial dependence specified according to a Gaussian Markov Random Field
(GMRF; (Lindgren et al., 2011); we refer to the two-step process of REVEALS-based estimation
130 followed by this spatial interpolation as the REVEALS-GMRF approach. REVEALS-GMRF has been
used to develop spatially continuous gridded vegetation reconstructions in Europe to assess vegetation-
132 climate feedbacks resulting from natural and anthropogenic land cover change (Strandberg et al., 2022b)
and to evaluate ALCC models (Kaplan et al., 2017) and dynamic vegetation models (Pirzamanbein et al.,
134 2020; Dallmeyer et al., 2023; Zapolska et al., 2023).

Here we adopt the REVEALS-GMRF approach to reconstruct land cover changes in North
136 America during the Holocene. This work relies on 1445 Holocene pollen records drawn from Neotoma
and its constituent database, the North American Pollen Database (NAPD), with a targeted data-
138 mobilization campaign employed to add more records to the NAPD for western North America. Using
these data, we reconstruct the fractional cover of 32 plant taxa and three land cover types (LCTs):
140 evergreen trees and shrubs (ETS), summergreen trees and shrubs (STS), and open vegetation/land (OVL,
including grasses, herbs, and low shrubs) from 12,000 years ago (12 ka) to present. We present the
142 Holocene vegetation reconstructions by working across scales, first describing continental-scale trends in
land cover, then shifting to several regional-scale case studies to show how the continental-scale trends
144 emerge from taxon-level dynamics that vary within and among regions, with respect to key taxa, drivers,
and resultant land-cover changes. We then zoom out to discuss the continental-scale drivers of Holocene
146 land cover change in North America and possible biophysical implications of these changes for Holocene
vegetation-atmosphere interactions and the Holocene Conundrum. Lastly, we discuss the potential
148 limitations of the REVEALS-GMRF approach and the opportunities now available for well-constrained
hemispheric- to global-scale studies of vegetation-atmosphere interactions.

150 2. Data and methods

2.1 Pollen data and data mobilization for western North America

152 Western North America has traditionally been underrepresented in the NAPD and Neotoma, but the
density of fossil pollen records in western North America has steadily increased in recent decades, as
154 multiple teams have worked to collect new records, often focusing on interactions among past vegetation,
fire, climate, and human dynamics (Anderson et al., 2008; Gavin and Brubaker, 2014; Marlon et al.,
156 2012; Iglesias et al., 2018; Alt et al., 2018). Many of these datasets were contributed to Neotoma



(Williams et al., 2018) when originally published, while others were contributed to Neotoma for an open-
158 data mobilization campaign conducted for this paper and PAGES LandCover6k (Gaillard et al., 2018).

After this effort, 1582 North American Holocene pollen records were downloaded from Neotoma
160 (Supp. Table 1). Each record included pollen count data at a series of depths. For methodological
consistency (Flantua et al., 2023), we refit all age-depth models using a custom-built workflow
162 (<https://github.com/andydawson/bulk-bchron>) that assessed chronological constraints and then used these
chronological constraints and IntCal20NH (Reimer et al., 2020) to fit the Bchron age-depth model
164 (Parnell et al., 2008). This resulted in 1445 records with age-depth models. Ages of the youngest and
oldest chronological constraints were used to determine the reliable age range for each record; we limited
166 extrapolation of pollen sample ages beyond the youngest or oldest constraints to 1000 years. Pollen types
were aggregated to taxa using the taxa list in the North American Modern Pollen Database (Whitmore et
168 al., 2005). We used a subset of 32 taxa for this analysis, choosing the most abundant taxa, several open-
land indicators, and taxa with available estimates of relative pollen productivity (Tables 2, 5).

170

2.2 REVEALS (regional reconstructions)

172 Pollen-based land cover reconstructions were performed using the REVEALS pollen-vegetation model
(Sugita, 2007b), and based on the standard protocol for PAGES LandCover6k (Trondman et al., 2015;
174 Githumbi et al., 2022a). This model estimates the relative abundance of plant taxa, along with the
standard error of these estimates, given pollen counts and input parameters that represent sedimentary
176 basin size and type, pollen productivity estimates (PPEs), pollen fall speeds, and atmospheric conditions.
REVEALS was developed to operate at the regional scale (Sugita, 2007a; Hellman et al., 2008a, b);
178 inferences of plant relative abundance represent the background vegetation over large areas (suggested as
100 km x 100 km in (Hellman et al., 2008b), but this scale is variable). REVEALS traditionally has been
180 used to infer plant relative abundance from records from large lakes (>50 ha), but has been tested and
applied to regions with records from a number of smaller lakes. The REVEALS model accounts for both
182 differential productivity and dispersal among taxa. Differential productivity is determined by taxon-
specific PPEs, while dispersal is modeled according to a Gaussian plume (Sutton, 1953) or Lagrangian
184 dispersal-deposition model (Kuparinen et al., 2007), both of which require the specification of
atmospheric conditions including wind speed. REVEALS accounts for differential dispersibility among
186 taxa using pollen fall speeds. See (Sugita, 2007b; Githumbi et al., 2022a) for a more detailed and
theoretical description of REVEALS. We implement REVEALS using the REVEALSinR R package
188 (Theuerkauf et al., 2016). REVEALS estimates for other regions included in the LandCover6k effort (Li
et al., 2023a; Githumbi et al., 2022a) were developed using more traditional implementations of this



190 model (LRA.REVEALS.v6.2.4.exe (Sugita, unpublished) and LRA R package (Abraham et al., 2014)),
which differ slightly in their calculation of the standard errors of relative abundances.

192 Pollen source areas and the relative representation of plant taxa in the REVEALS dispersal-
deposition model are affected by sedimentary basin type (e.g. lake, mire) and area (Sugita, 2007a;
194 Trondman et al., 2016). Basin type is typically included in Neotoma metadata for pollen datasets, but not
all datasets include metadata on basin area. To determine basin area for these datasets, we developed a
196 standard workflow (Goring, 2021); https://github.com/NeotomaDB/neotoma_lakes). First, we used
hydrological databases (National Hydrography Dataset (United States Geological Survey, 2022), National
198 Hydro Network (Natural Resources Canada, 2022)) to assign basin areas to datasets whose coordinates
fell within a water-body polygon. Second, for dataset coordinates that landed outside a water-body
200 polygon, we used Google Earth Engine to identify the basin. These basins were traced using the polygon
tool in Google Earth Engine, and basin area was calculated from polygon area. Not all basins could be
202 identified, however, particularly for pre-GPS sites in Neotoma with imprecise coordinates. Third, for sites
still without basin area, we assigned a size of 50 ha. In the context of the REVEALS model, this
204 represents a medium-sized lake. This decision avoids the potential biases from assigning large or small
lake areas, although site-level reconstructions may over- or under-represent taxa if basin area (and hence
206 pollen source area) is inaccurate (Jackson, 1990; Davis, 2000; Liu et al., 2022). All basin areas recovered
in the first and second steps were added as site-level metadata to Neotoma, along with dataset notes.

208 We used PPE and fall speed datasets from Wieczorek and Herzschuh (2020) for the Northern
Hemisphere extra-tropics. Specifically, we used the North America continental-scale datasets, which
210 include PPE (with grass as the reference taxon) and fall speed values for 30 of the 32 taxa we consider in
this work. For *Ambrosia* (ragweed) and *Tsuga* (hemlock), which were not included in Wieczorek and
212 Herzschuh (2020), we use PPE and fall speed values from a previously compiled North America dataset
(Dawson et al., 2016; Trachsel et al., 2020). Additionally, for the *Larix* (larch) fall speed, we used the
214 value for *Larix laricina* from (Niklas, 1984), which is the dominant species in eastern and northern North
America. This estimate is an order of magnitude smaller than the *Larix* taxon-level fall-speed estimate
216 included in (Wieczorek and Herzschuh, 2020), which originates from (Bodmer, 1922)). We experimented
with fall-speed datasets that included these larger *Larix* fall-speed estimates; these vegetation
218 reconstructions indisputably overrepresented larch.

 We used the Gaussian plume dispersal model with a wind speed of 3 m/s and neutral atmospheric
220 conditions (vertical diffusion coefficient $c_z=0.12$; turbulence parameter $n=0.25$; wind speed $u=3$ m/s; see
(Jackson and Lyford, 1999a)), to be consistent with the dispersal model specified in the LandCover6k
222 protocol for Northern Hemisphere reconstructions (Dawson et al., 2018; Githumbi et al., 2022a). We set



224 the region cutoff to the REVEALSinR function default of 100 km; this specifies the maximum distance
that most pollen will originate from (Sugita, 2007a; Theuerkauf et al., 2016).

226 We reconstructed land cover for 25 time intervals that cover the Holocene. These time intervals
were defined according to the LandCover6k working group protocol (Trondman et al., 2015) (SI Table
4). Time intervals are specified in kiloyears before present (ka), where present is defined as 1950 CE, but
228 for time intervals <1ka we also note the Common Era (CE) timescale. Intervals in the period from 11.7 to
0.7 ka have a 500-year temporal grain (11.7 to 11.2 ka; 11.2 to 10.7 ka; etc.), while the three most recent
230 intervals have a finer temporal grain (0.7-0.35 ka [1250-1600 CE]: 350 years; 0.35-0.1 ka [1600-1850
CE]: 250 years; 0.1-(-0.074) ka: 174 years [1850-2024 CE]) in order to better capture the changes
232 associated with intensifying anthropogenic land use over the last five centuries. Pollen samples were
assigned to a time interval based on their mean calibrated radiocarbon age. If multiple samples for a
234 record fell within the same interval, pollen counts were summed by taxon, so that each record would have
at most one set of pollen counts per time interval. We used a grid resolution of $1^\circ \times 1^\circ$, also as specified by
236 the LandCover6k protocol. Within a grid cell, REVEALS reconstructions for multiple sites were
averaged, as is standard practice (Sugita, 2007a). Taxon-level reconstructions were aggregated to three
238 land cover categories (SI Table 5): summergreen trees and shrubs (STS), evergreen trees and shrubs
(ETS), and open vegetation/land (OVL), which includes grasses, herbs, and low-stature shrubs. All trees
240 and shrubs (ATS) is calculated as the sum of STS and ETS.

242 **2.3 REVEALS-GMRF (spatial modeling and interpolation with uncertainty)**

Here, we use the REVEALS-GMRF Bayesian hierarchical model (Pirzamanbein et al., 2018b) to spatially
244 interpolate the REVEALS-based land cover reconstructions. REVEALS-GMRF exploits the spatial
dependence in land cover using a Gaussian Markov Random Field, and permits the characterization of
246 uncertainty given the empirical land cover product. As in Pirzamanbein et al. (2018), we use elevation as
a covariate. Although including simulations of land cover as an additional covariate can further improve
248 the reliability of resulting land cover maps (Pirzamanbein et al., 2020), the intent of our work is to
develop a spatial land cover product suitable for validation of and assimilation with dynamic vegetation,
250 land use, and Earth System models. Hence, to maintain independence, we refrain from using simulated
land cover as a covariate. To quantify overall uncertainty of a grid cell for a specified time period, we
252 computed the area of confidence regions (CR; (Pirzamanbein et al., 2018a)). Smaller CR values indicate
higher confidence, while larger CR values indicate more uncertainty. As in Pirzamanbein et al. (2018), a
254 CR threshold is determined using the complete set of CR values. Accordingly, any grid cells with a CR
greater than a threshold of 9 were omitted from spatial reconstructions (Githumbi et al., 2022c). The



256 result of this spatial interpolation is a set of empirically-based land cover maps for North America and the
257 LandCover6k time intervals, with uncertainty.

258

2.4 Calculation of proportional changes and mapped anomalies

260 To summarize continental-scale land-cover dynamics through time, we built time series of both mean
261 relative cover and area-weighted relative cover. We used recently updated ice sheet maps (Dalton et al.,
262 2020) to identify glaciated and unglaciated grid cells for each time period, then calculated the fraction of
263 unglaciated land cover for each time period. We then calculated the mean relative cover of each land
264 cover type for each time period, across all unglaciated grid cells at that time period. Mean relative cover
265 usefully summarizes land cover change within ice-free regions, but does not track the overall increases in
266 vegetated land area in North America during the last deglaciation. To calculate area-weighted relative
267 cover, for each time period, we multiplied the relative cover of each grid cell by the cell area, and then
268 summed the relative cover of each land cover type across space for unglaciated land grid cells. We then
269 divided these summed area-weighted cover values for each time period by the sum of total unglaciated
270 land area at 0.25 ka. Because the number of unglaciated land grid cells changes through time, while the
271 denominator is constant, this area-weighted metric of relative cover is affected by both available land and
272 changes in land cover proportion, resulting in a proportional metric that is sensitive to continental-scale
273 increases in vegetation cover.

274 For each pair of time intervals, we calculated land cover change as grid-cell scale differences for
275 each of the three land cover classes. After visually identifying areas of large land cover changes (Supp.
276 Fig. 3), we identified several regions for further investigation: the northeastern US and southeastern
277 Canada (NEUS/SEC), eastern Canada (ECAN), western Canada and Alaska (WCAN/AK), and the
278 Pacific Coast, Cascades, and Sierra Nevada (PCCS) based on areas of greatest change and pollen-site
279 density. We then assessed vegetation change for each region at both the taxon and land cover scales,
280 using the REVEALS grid-cell estimates of taxon mean abundances and the REVEALS-GMRF
281 interpolated estimates of mean cover for the land cover types.

282 3. Results

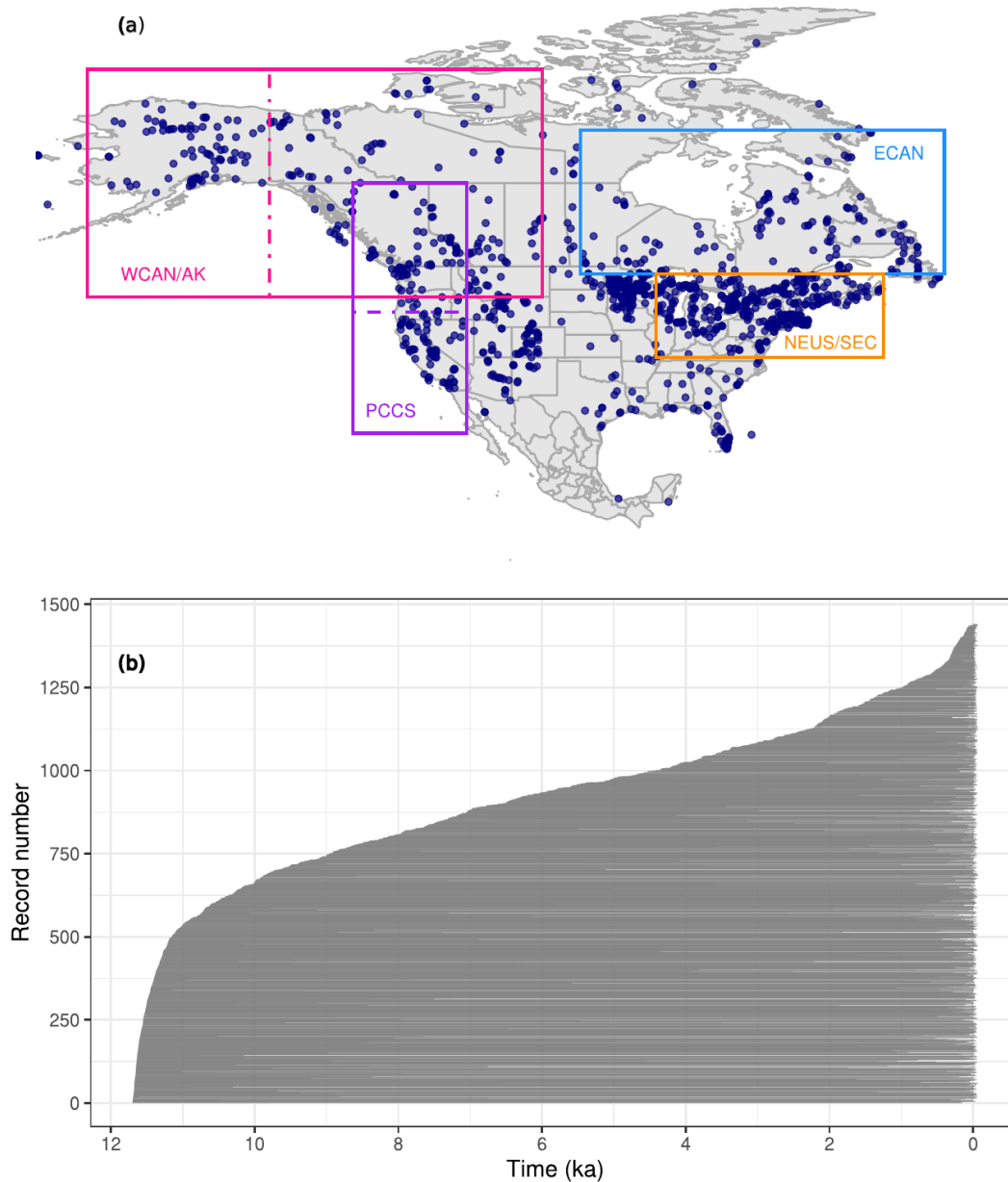
3.1 Data coverage

284 The assembled dataset of 1445 fossil pollen records has good coverage across the continental US and
285 Canada (Fig. 1a). Areas of relatively high site density include the Great Lakes region of the US and
286 Canada, the northeastern US, the Rocky Mountains, the Pacific Coast, and central Alaska. Given good
287 data-mobilization efforts for the US and Canada, this distribution reasonably approximates the true



288 distribution of fossil pollen records, so spatial gaps usually represent lack of available sites (e.g. few lakes
or wetlands in arid regions) or inaccessibility (e.g. high Arctic). Conversely, a lower site density in
290 Mexico and Central America is partially due to less extensive open-data mobilization efforts in these
regions. Temporally, the distribution of oldest samples (an indicator of record length) is smooth (Fig.
292 1b), with rapid accumulation of sites between 11.7 and 11 ka (33% of sites have an oldest sample in this
interval) and between 0.5 and -0.074 ka (74% of sites have a youngest sample in this interval).

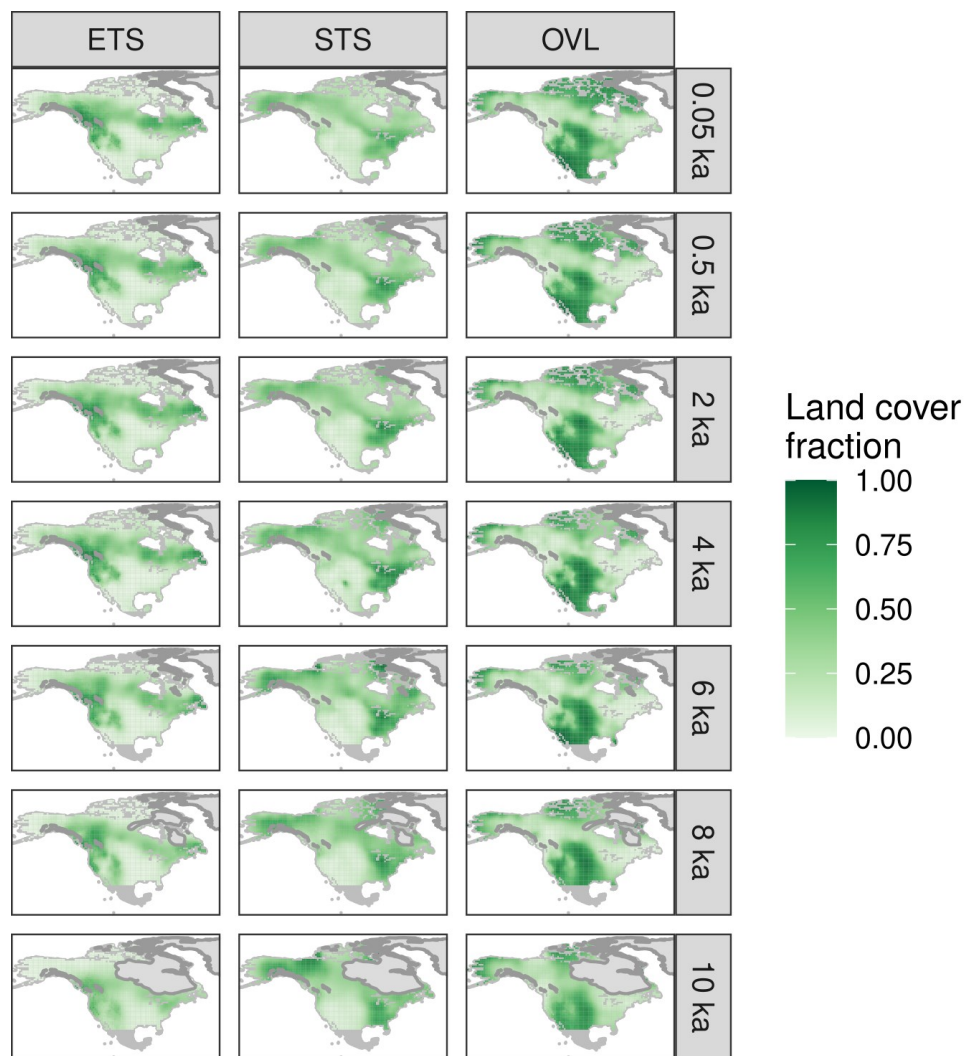
294



296 **Figure 1:** The spatiotemporal distribution of fossil pollen data used here. A) Map indicating the spatial
298 distribution of sites recovered from the Neotoma Paleocology Database, as well as the case study regions
(WCAN/AK: Western Canada and Alaska; PCCS: Pacific Coast, Cascades, and Sierra Nevada; ECAN:
Eastern Canada; and NEUS/SEC: North-Eastern US and South-Eastern Canada). B) Temporal extent of



300 all sites, in which each site is represented by a horizontal gray line between the site's oldest and youngest
Holocene samples. Sites are ordered by age of the oldest sample, reported as ka. Samples older than 11.7
302 ka are not shown.



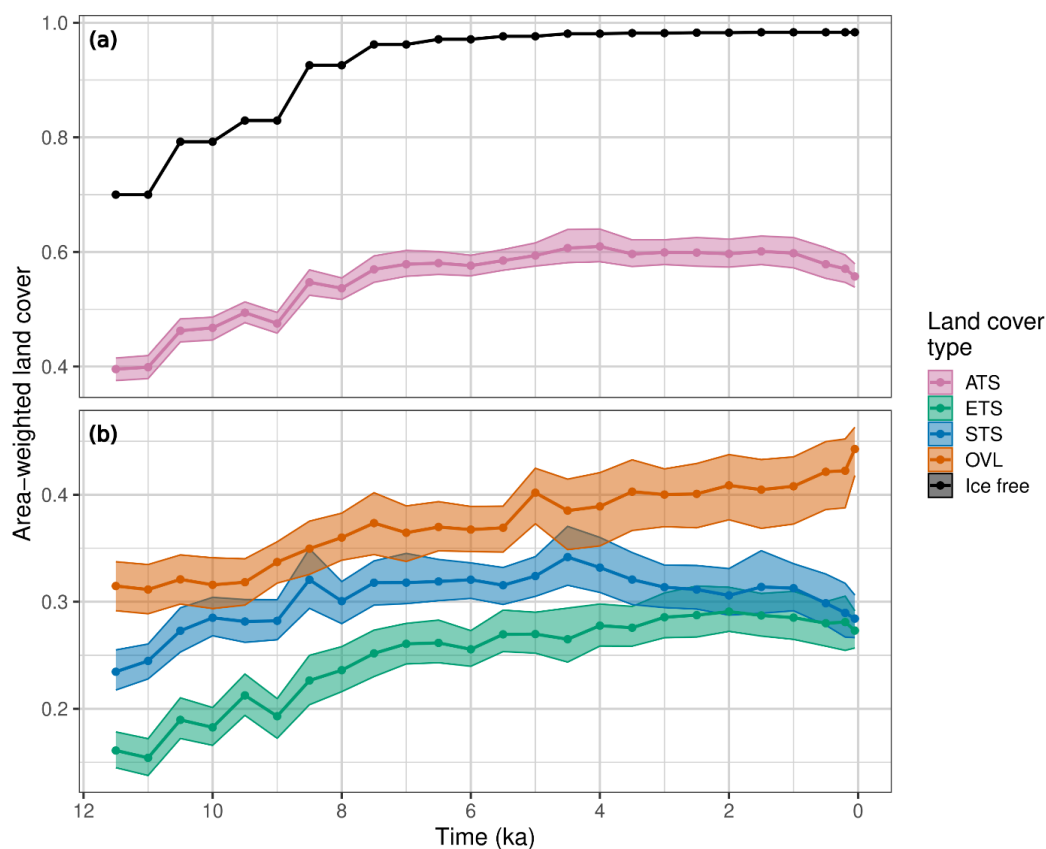
304

306 **Figure 2:** Interpolated REVEALS-based estimates of fractional cover for evergreen trees and shrubs
308 (ETS), summergreen trees and shrubs (STS), and open land (OVL). Laurentide and Cordilleran Ice Sheet
extents (Dalton et al., 2020) are indicated by gray polygons. Estimates are presented on a $1^\circ \times 1^\circ$ grid, for
selected time periods, with ages reported as ka. Map ordering follows the geological convention of oldest



310 maps at bottom. The spatial domain for interpolation includes all unglaciated locations in North America
between 17 and 79°N.

312



314

Figure 3: (a) Holocene trends in area-weighted cover of all trees and shrubs (ATS) in North America
316 (pink curve with 95% uncertainty envelope), expressed relative to present unglaciated land area (see
Methods), and the fraction of unglaciated land relative to continental land area (black). Total cover is the
318 sum of the evergreen and summergreen trees and shrubs. (b) Trends in the area-weighted cover of
evergreen (ETS), summergreen (STS) and open vegetation/land (OVL) for North America. For both plots,
320 land cover estimates are based on the interpolated data for the spatial domain shown in Fig. 2.

322

3.2 Continental-scale trends in Holocene land cover



324 At a continental scale, the spatial configuration of land cover in North America has been broadly stable
during the Holocene (Fig. 2). Persistent features include belts of high evergreen tree cover in the
326 mountainous West and Canada, high summergreen tree cover in the eastern US, moderate to high cover of
summergreen trees and shrubs in Alaska and northern Canada, and high proportions of open vegetation in
328 the Great Plains, western Alaska, and Arctic Canada (Fig. 2).

However, despite this broadly stable spatial configuration, there were large continental-scale
330 changes in the area-weighted fractional cover of land cover types in North America during the Holocene,
particularly during the early Holocene (Fig. 3a, Supp. Fig. S3). From 11.7 to 7 ka, the area-weighted
332 fraction of forested land cover increased from about 56 to 91%. This increase closely tracked the
increase in available land surface area, as the Laurentide Ice Sheet retreated (Fig. 3a) (Dalton et al., 2020).
334 During the early Holocene, the largest gains in forest cover were across deglaciated western Canada and
ice-marginal areas in eastern Canada (Fig. 2, Supp. Fig. S3). Forest cover continued to expand between
336 7.5 and 4.5 ka (Fig. 3a), even though the Laurentide Ice Sheet had disappeared by ~6 ka, with the largest
afforestation in the northern Great Plains of central Canada and in recently deglaciated regions of eastern
338 Canada (Fig. 2, Supp. Fig. S3). Continental-scale forest cover remained stable from 4.5 to 1.5 ka, then
declined after 1.5 ka (Fig. 3a). The late-Holocene decline in forest cover was most pronounced in the
340 eastern US and in Arctic and boreal Canada where open vegetation began increasing after 4 ka (Fig. 2,
Supp. Fig. S3, S4).

342 Within these Holocene trends, the three land cover types followed differing trajectories (Fig. 3b).
All three show a strong increase between 11.7 and 7.5 ka in their area-weighted relative cover, again
344 tracking ice retreat. After 7.5 ka, however, the three trajectories diverged. Evergreen trees and shrubs
continued to rise slowly but steadily from 7.5 to 2 ka, then declined slightly (Fig. 3b). Summergreen trees
346 and shrubs reached peak area-weighted cover at 4.5 ka, then declined, with an accelerated decline after
1.5 ka. The proportion of open lands remained largely stable from 7.5 to 4.5 ka, then increased, with an
348 accelerating increase after 2 ka. A close examination of the continental-scale anomaly maps (Supp. Figs.
S3, S4) suggests a fairly complex spatial mosaic for each land cover type, with the continental-scale
350 trends emerging from a welter of regional-scale phenomena. For example, widespread gains in evergreen
trees and shrubs across much of Canada and Alaska between 6 and 4 ka were partially offset by large
352 losses in the eastern US and southeastern Canada over the same period (Supp Fig. S3). Because different
plant species predominate in different regions of North America, these continental-scale trends in land
354 cover were the emergent outcomes of individualistic species-level responses to changing climates and, in
some places, intensifying land use (Williams et al., 2004).

356



358 3.3 Regional case studies

359 3.3.1 Northeastern US & Southeastern Canada (NEUS/SEC)

360 For the mostly forested NEUS/SEC, after initial afforestation and loss of open lands during the early
361 Holocene (10 to 8 ka), the central dynamic has been shifts in the relative cover of evergreen and
362 summergreen trees and shrubs (Fig. 4a, Supp. Fig. S5). The fractional cover of evergreen trees and shrubs
363 declined throughout the early to middle Holocene (10 to 4 ka) in the southern part of the domain, which
364 intensified to widespread loss across the NEUS/SEC (6 to 4 ka), but then reversed after 4 ka, with
365 recovery and regrowth of evergreen trees and shrubs (Fig. 4a). The western increase in open lands
366 between 8 and 4 ka is caused by the eastward expansion of prairie due to drier conditions (Williams et al.,
367 2009b), while the decrease in open lands from 4 to 0.5 ka is due to increased moisture availability that
368 resulted in a westward shift of the prairie-forest border and increase in summergreen forest taxa in the
369 eastern Midwest (Umbanhowar et al., 2006). Overall, the low proportions of open vegetation in the
370 NEUS/SEC from 9 ka until European settlement (Fig. 4B) likely represents these western prairies and
371 local wetlands, which expanded in the late Holocene in parts of the NEUS/SEC (Brugam and Swain,
372 2000; Ireland and Booth, 2010), rather than grasslands or other open lands in eastern deciduous forests
(Faison et al., 2006).

374 At a taxon level, most changes in evergreen cover can be attributed to regional declines of cold-
375 tolerant conifers such as *Picea glauca*, *P. mariana*, and *P. rubens* (white, black, and red spruce); *Pinus*
376 *banksiana*, *P. resinosa*, and *P. strobus* (jack, red, and white pine), and *Abies balsamea* (balsam fir)
377 between 10 and 6 ka (Fig. 4c, Supp. Fig. S6) (Spear et al., 1994; Jackson and Whitehead, 1991; Jackson
378 et al., 1997). These changes, combined with the zonal pattern of evergreen expansion in the northern
379 NEUS/SEC and declines in the southern part, suggest that much of the evergreen tree and shrub cover
380 changes during the early to middle Holocene can be attributed to postglacial northward shifts in tree
distributions in response to rising temperatures and deglaciation.

382 A second major feature is the well-known and dramatic expansion, collapse, and re-expansion of
Tsuga canadensis (eastern hemlock), a cool-temperate conifer that typically occupies warmer climates
384 than *Abies balsamea* (Thompson et al., 1999). Investigations continue into understanding the abrupt and
widespread collapse in *Tsuga canadensis*, which differed from the overall evergreen trend. The collapse
386 occurred in less than 10 years at some sites (Allison et al., 1986) and is linked to regional shifts in water
availability and temperature gradients (Booth et al., 2012; Foster et al., 2006; Haas and McAndrews,
388 1999; Shuman et al., 2023). Initial hypotheses that a pest or pathogen such as hemlock looper (Bhiry and
Filion, 1996; Davis, 1981; Anderson et al., 1986) caused the hemlock decline have not been supported by
390 recent investigations (Oswald et al., 2017), although insect remains are scarce in lacustrine archives.
Understanding the causes of the hemlock collapse is outside the scope of this paper; however, this paper

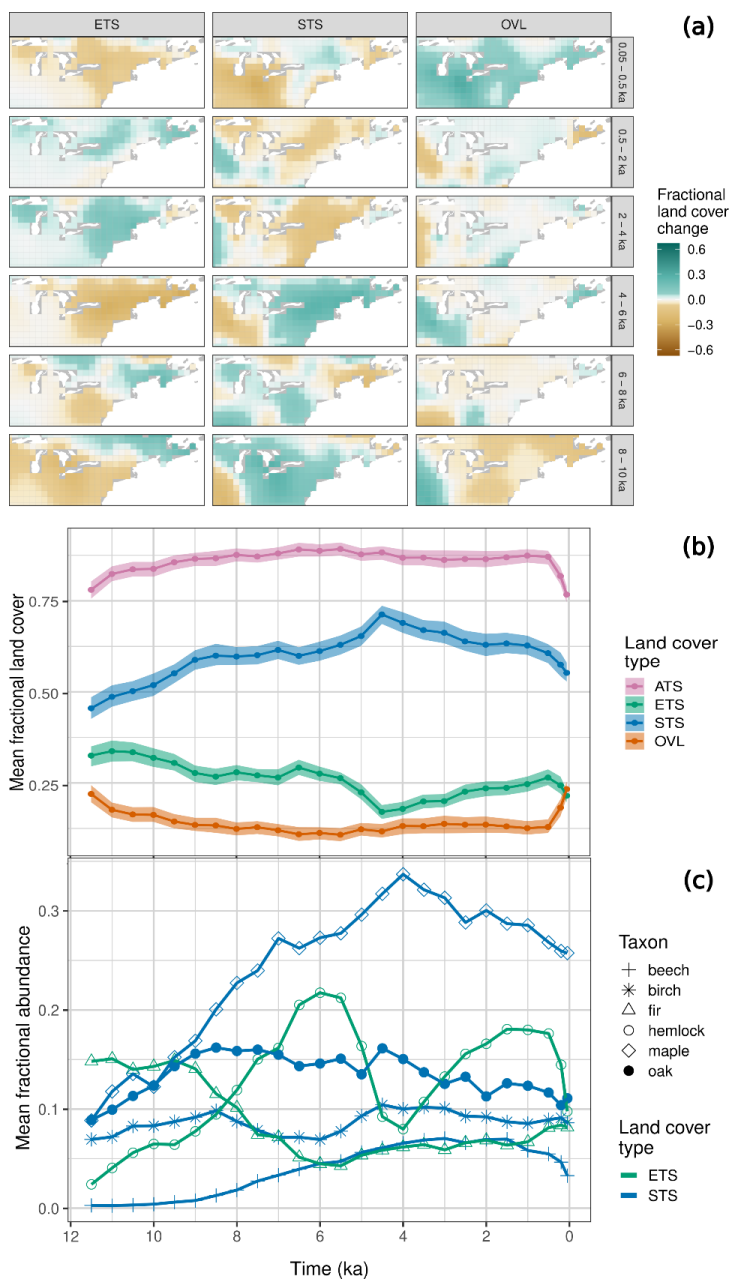


392 shows its importance, in that a single-species collapse fundamentally altered the functional composition,
ecosystem phenology, and land cover of the NEUS/SEC for thousands of years.

394 Among summergreen taxa, these REVEALS reconstructions indicate a strong growth in *Acer*
(maple) cover in the NEUS/SEC until 4 ka and declines thereafter. *Acer saccharum* (sugar maple) is
396 probably the dominant taxon driving this curve, with *A. rubrum* (red maple) increasing in the late
Holocene (Finkelstein et al., 2006). *Quercus* (oak) abundances were high between 9 and 4.5 ka, then
398 steadily declined, while *Betula* (birch) abundances remained relatively stable. *Fagus grandifolia*
(American beech) abundances continued to steadily increase throughout this period until 3 ka, then began
400 declining after 1.5 ka, along with *Tsuga canadensis*, while *Abies balsamea* abundances increased.
Disturbance-related taxa and indicators of open vegetation such as *Ambrosia* (ragweed) and *Rumex*
402 (sorrel, not shown) begin increasing at ca. 0.35 ka (1600 CE). These late-Holocene changes in forest
composition can be plausibly attributed to regional cooling (explaining the increase in *Abies balsamea*)
404 and perhaps also intensified human land use and disturbance, with the relative importance of these drivers
varying at subregional scales and among taxa (Oswald et al., 2020; Mottl et al., 2021).

406 An intriguing feature of these REVEALS reconstructions is the inference of *Abies balsamea* and
Acer spp. as the most common evergreen and summergreen tree taxa in the NEUS/SEC, given that *Picea*,
408 *Pinus*, and *Quercus* are more abundant in pollen and macrofossil records and prior site-level and regional
syntheses of Holocene pollen records have emphasized their dynamics (Jackson et al., 1997; Jackson and
410 Whitehead, 1991; Payette et al., 2022; Spear et al., 1994). Witness-tree data in the NEUS also indicate
that *Fagus* and *Quercus* were the most abundant broadleaved taxa at time of European settlement
412 (Thompson et al., 2013). One possible reason for the higher levels of *Abies* and *Acer* reported here is
that our NEUS/SEC domain extends a bit farther north than prior reconstructions that have focused more
414 on central and southern New England. A second possibility is that the parameterizations for *Abies* and
Acer are incorrect, causing the coverages of these taxa to be overestimated (see Discussion).

416



418 **Figure 4:** (a) Land cover anomaly maps for the northeastern US and southeastern Canada
420 (NEUS/SEC) case-study region. Maps show the anomalies in fractional cover for each land
cover class for pairs of indicated time intervals. Spatial resolution is $1^{\circ} \times 1^{\circ}$ and time units are ka.
(b) Holocene trends in the mean relative cover of the three land cover types (ETS, STS, OVL)



422 and the ATS sum for the uninterpolated REVEALS grid cell estimates across the NEUS/SEC
423 region. (c) Holocene trends for the REVEALS abundance estimates for the six most commonly
424 occurring taxa in the region. Line color indicates assignment of individual taxa to land cover
425 types. For taxon-level maps, see Supp. Fig. 6.

426

3.3.2 Eastern Canada (ECAN)

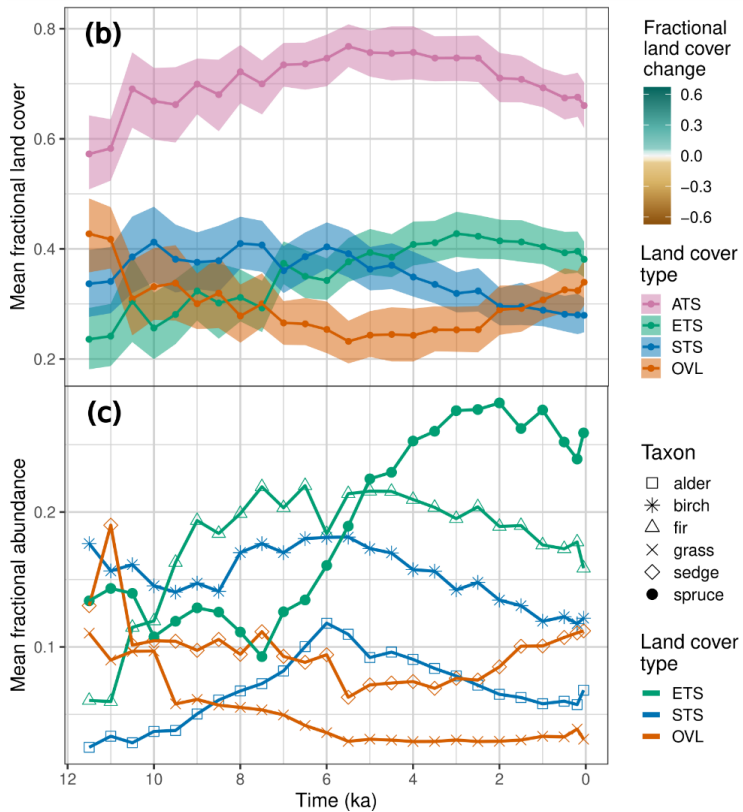
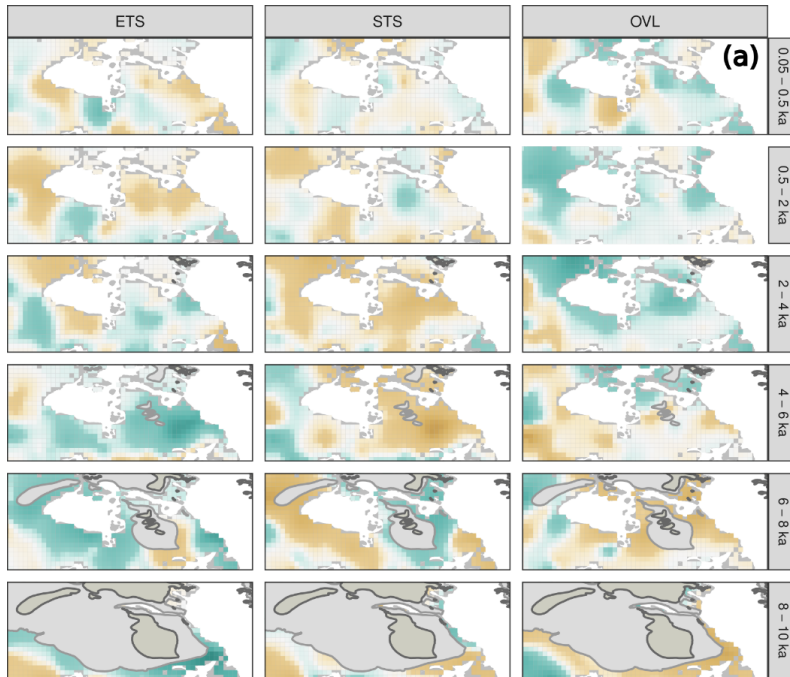
428 In Eastern Canada (ECAN), immediately north of the NEUS/SEC, evergreen trees and shrubs expanded
429 across the entire region until 4 ka, with slower and more spatially heterogeneous expansion of evergreen
430 cover between 4 and 2 ka (Fig. 5a, Supp. Fig. S7). After 4 ka, open vegetation expanded (Fig. 5a, 5b).
431 This expansion of evergreen trees and shrubs can be traced to separate phases of expansion for *Abies*
432 *balsamea* and *Picea*, with *A. balsamea* expansion mostly between 11.5 and 7.5 ka (in the southern
433 portion) and *Picea* expansion mostly between 7.5 and 3 ka, across the area and especially in the central
434 portion (Fig. 5c, Supp. Fig. S8). Increasing Cyperaceae abundance after 3.5 ka signal the expansion of
435 forest-tundra. Major hardwood summergreen taxa include *Betula* and *Alnus*. *Alnus* abundances expanded
436 until 6 ka, then slowly declined, while birch abundances expanded between 8.5 and 6 ka, then also
437 declined. These declines in *Alnus* and *Betula* after 6 ka co-occurred with expansions of *Picea* and
438 Cyperaceae, suggesting that the regional vegetation shifted from more of a mixed forest or woodland in
439 the early Holocene, to evergreen coniferous forest, forest-tundra, or tundra in the middle to late
440 Holocene. Note that *Populus* is not included in these REVEALS reconstructions, but it is an important
441 taxon in ECAN (Peros et al., 2008), and its omission may cause an underestimate of summergreen cover.

442 These vegetation changes in ECAN can be attributed to a combination of deglaciation, changing
443 temperatures, and fire history. The Laurentide Ice Sheet collapsed at 8.4 ka and the last remnants of the
444 Labrador Dome disappeared from northern Quebec by 5.7 ka (Dalton et al., 2020). The replacement of
445 open land by forest cover during the early Holocene was driven primarily by increases in evergreen trees
446 and shrubs. The open forests at this time lack modern analogues and varied spatially in taxonomic
447 composition, with more fir and birch to the east and spruce toward the west (Richard et al., 2020). By 7.5
448 ka, closed forests developed in response to warmer temperatures. This was followed by a decrease in
449 summergreen taxa in the southern portion of the boreal forest as well as a decline in fir in the lichen
450 woodland and feathermoss forest toward the west (Fréchette et al., 2021; Richard et al., 2020). In the
451 lichen woodlands of the north, shrub birch and paper birch decreased after 6ka, although remaining high
452 in the southwest (Fréchette et al., 2018). Near treeline, spruce forests were more open between 7 and 4 ka,
453 with *Alnus* and shrub *Betula* more abundant (Fréchette et al., 2018; Gajewski, 2019). In ECAN, spruce
454 abundances reached a maximum between 4 and 2 ka (Fréchette et al., 2018), with the southern portion of
the forest tundra becoming lichen woodland at this time. After 2 ka, *Picea* abundances at northern sites



456 declined and open lands increased in response to cooling, but the timing and rate of *Picea* losses varied
among sites and is governed in part by fire history (Gajewski et al., 2021; Gajewski, 2019).

458



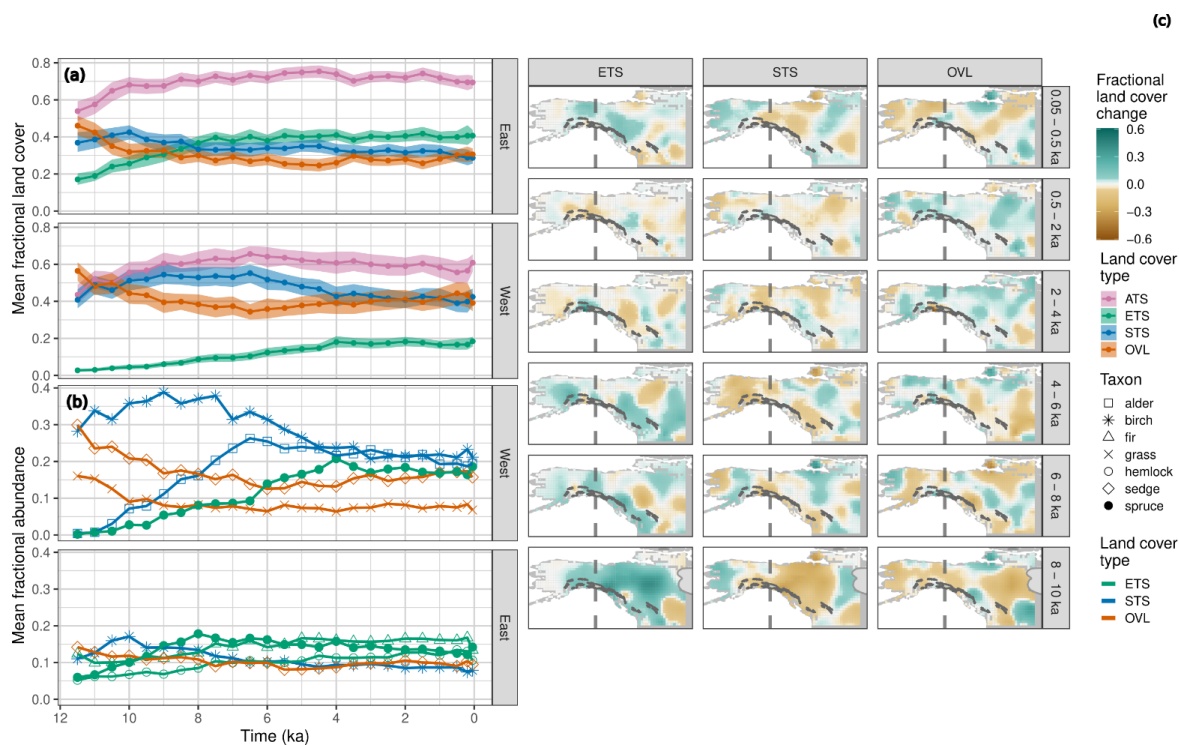


460 **Figure 5:** (a) Land cover difference maps for ETS, STS, and OVL for the eastern Canada (ECAN) case
study. (b) Holocene trends in the mean relative cover of the three land cover types (ETS, STS, OVL) and
462 the ATS sum for the uninterpolated REVEALS grid cell estimates across the ECAN region. (c) Holocene
trends for the REVEALS abundance estimates for the six most commonly occurring taxa in the region.
464 For both panels, figure conventions follow Figure 4. For taxon-level maps, see Supp. Fig. 8.

466 3.3.3 Western Canada and Alaska (WCAN/AK)

In western Canada and Alaska (WCAN/AK), evergreen trees and shrubs rapidly expanded between 11
468 and 8 ka, while the coverage of summergreen trees and shrubs and open lands decreased (Fig. 6a, 6b,
Supp. Fig. S9). Most of Alaska was not glaciated during the Last Glacial Maximum; however, much of
470 western Canada, the Brooks Range in Alaska, and south-coastal Alaska were covered by ice (Dalton et
al., 2020). Evergreen tree species such as *Picea glauca* (white spruce) persisted in this region in local
472 microrefugia (Anderson et al., 2006), then expanded their ranges during end-Pleistocene warming and
deglaciation. Other evergreen taxa such as *Pinus contorta* expanded northward with deglaciation
474 (MacDonald and Cwynar, 1991). Trends in taxon abundances differ substantially between the western
and eastern subregions (Fig. 6c, Supp. Fig. S10). In the eastern subregion, changes in taxon abundances
476 were muted, with a modest expansion in *Picea* and *Tsuga* between 11.5 and 7.5 ka, and a slow decline in
Betula between 10 and 6 ka. *Tsuga* (mostly *Tsuga heterophylla*; western hemlock) occurs primarily along
478 the coast, was abundant along the south coastal areas by 11 ka (Lacourse et al., 2012; Lacourse and
Adeleye, 2022), arrived by 9.5 ka into southeast Alaska (Hansen and Engstrom, 1996; George et al.,
480 2023), increased in abundance along the south-coastal areas by 8 ka, and then expanded during the mid-
to late Holocene into south-central Alaska (Anderson et al., 2017) and the inland mesic forests of British
482 Columbia (Rosenberg et al., 2003; Gavin et al., 2021). In the western part of this domain (mainly
Alaska), changes in summergreen hardwood (mostly shrub) taxa predominate, with a major expansion of
484 *Alnus* between 11.5 and 6.5 ka (Anderson and Brubaker, 1994; Cwynar and Spear, 1995), and a modest
expansion of *Betula* between 11.5 and 9 ka. These expansions were accompanied by declines in Poaceae
486 and Cyperaceae, with continued decline in Cyperaceae until 6 ka. *Picea* abundances steadily increased
until 4 ka. The net effect was a decline in open vegetation and expansion of evergreen and summergreen
488 trees and shrubs during the early to middle Holocene, with apparent region-wide stability after 4 ka
(Anderson et al., 2019).

490



492

Figure 6: (a) Land cover difference maps for the western Canada / Alaska (WCAN/AK) case study
494 region. (b) Holocene trends in the mean relative cover of the three land cover types (ETS, STS, OVL) and
the ATS sum for the uninterpolated REVEALS grid cell estimates across the WCAN/AK region, with
496 grid cells averaged separately for eastern and western subregions (dividing line shown in (a) as vertical
dashed line). (c) Holocene trends for the REVEALS abundance estimates for the six most commonly
498 occurring taxa in the region, with grid cells averaged separately for eastern and western subregions. For
both panels, figure conventions follow Figure 4. For taxon-level maps, see Supp. Fig. 10.

500

3.3.4 Pacific Coast, Cascade, and Sierra Nevada Ranges (PCCS)

502

In contrast to the other regions, evergreen trees have dominated much of the land cover in the PCCS
region since 12 ka (Fig. 7a, 7b, Supp. Fig. S11). In the northern subregion (often referred to as the Pacific
504 Northwest), the proportions of cover types were fairly constant until 9 ka, after which summergreen and
open land declined until 6 ka (Fig 7a, 7b). However, taxon-level changes were very dynamic. From 11.7
506 to 10.5 ka, the REVEALS-estimated abundance of *Pseudotsuga menziesii* (Douglas-fir) more than
doubled, reflecting its arrival, expansion, and northward migration (Gugger and Sugita, 2010), and
508 replacing true firs (*Abies*) and *Picea* (Fig 7c, Supp. Fig. S12). In the coastal ranges, frequent forest fires
in the early Holocene contributed to a *Pseudotsuga-Alnus rubra* association in the mountains (Gavin et



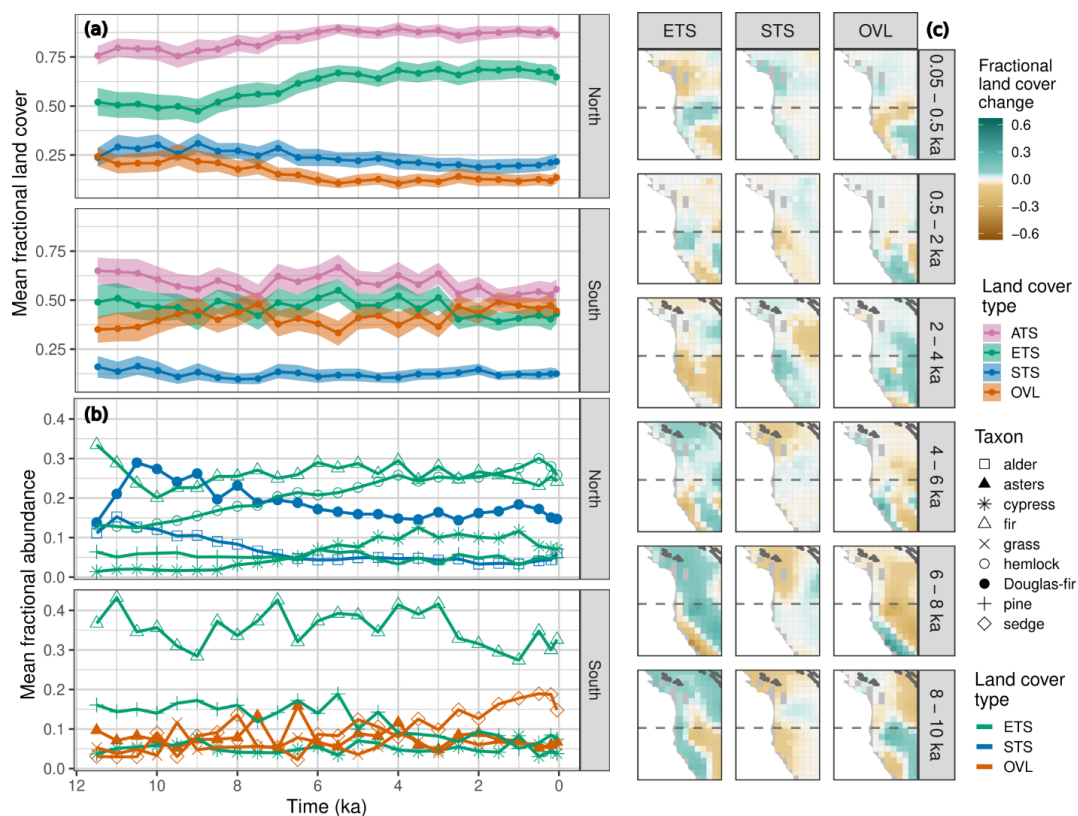
510 al., 2013; Long et al., 1998, 2007) and an oak savanna (not shown) that was common in the lowlands
512 (Walsh et al., 2008, 2010; Giuliano and Lacourse, 2023). Summergreen taxa (mostly *Alnus rubra*) and
open-land pollen indicators declined from 8 to 6 ka (Fig 7b), replaced by shade-tolerant *Abies*, *Tsuga*, and
514 Cupressaceae, which is mostly western redcedar in this region (Fig. 7b) (Lacourse, 2009; Gavin et al.,
2013; Worona and Whitlock, 1995). After 6 ka, the overall abundance of conifer taxa remained constant
516 (Fig 7a, 7b), although the proportion of hemlock and cedar increased steadily through the late Holocene
while *Pseudotsuga* declined, consistent with less fire and the persistence of old-growth forest (Whitlock,
1992; Lacourse and Adeleye, 2022), until the logging of the last century, which manifested as a decline in
518 conifer and increase in summergreen and open land in the coastal forests (Fig. 7a) (Davis, 1973; Whitlock
et al., 2018).

520 The most common taxon in these REVEALS reconstructions, *Abies*, varied little over the last 9
ka, but this genus represents several shade-tolerant species (*A. lasiocarpa* [subalpine fir], *A. grandis*
522 [grand fir], *A. amabilis* [Pacific silver fir], *A. procera* [noble fir]) that collectively are common throughout
the region. As noted for the NEUS/SEC, the reconstructed values of *Abies* are likely too high, because
524 REVEALS estimate of fall speed is overestimated. *Pinus* also represents several species and was most
abundant in the dry eastern areas where it was consistently abundant during the Holocene (Minckley et
526 al., 2007). *Pseudotsuga* and *Larix* have indistinguishable pollen morphologies and are therefore grouped
in the reconstructions; however, *Larix* is limited to the eastern edge of this region.

528 The southern subregion (the Sierra Nevada, Klamath Mountains and California Coast ranges and
interior Great Basin) supported roughly equal amounts of conifer forest and open land that overall had
530 minor relative changes over the Holocene (Fig. 7a). Summergreen trees and shrubs have been infrequent
contributors to land cover in this subregion. At the taxon-level, *Abies* is again the most common
532 component of reconstructed evergreen land cover across the region, although its abundance may be
overrepresented in this parameterization of REVEALS (Fig. 7b). *Pinus* and *Quercus* were most abundant
534 in the early Holocene, forming open forests and woodlands, especially in the Klamath Mountains and
Sierra Nevada (Anderson, 1996; Briles et al., 2008) fire-prone forests east of the Cascade Range (Walsh
536 et al. 2015);. Most of the eastern portion of this subregion is the Great Basin shrub steppe, where the few
pollen records that exist are from high-elevation sites and low-elevation wetlands that are sensitive to
538 fluctuating water tables, recorded as large fluctuations in Cyperaceae pollen. Increases in open-land cover
taxa (Cyperaceae, Poaceae, Asteraceae) between 10-7.5 ka and after 3 ka in this region may reflect either
540 local expansion of alpine meadows and wetlands or expansion of steppe more broadly (Mensing et al.,
2008; Brugger and Rhode, 2020; Minckley et al., 2007; Thompson, 1992). Note, however, that desert,
542 steppe, and other open-land arid ecosystems are likely to be underrepresented in these reconstructions,
due to a scarcity of dryland sites.



544



546 **Figure 7:** (a) Land cover difference maps for the Pacific Coast, Cascade and Sierra Nevada (PCCS) case
 548 study region. (b) Holocene trends in the mean relative cover of the three land cover types (ETS, STS,
 550 OVL) and the ATS sum for the uninterpolated REVEALS grid cell estimates across the PCCS region,
 552 with grid cells averaged separately for northern and southern subregions (dividing line shown in (a) as
 554 vertical dashed line). (c) Holocene trends for the REVEALS abundance estimates for the six most
 commonly occurring taxa in the region, with grid cells averaged separately for northern and southern
 subregions. For both panels, figure conventions follow Figure 4. For taxon-level maps, see Supp. Fig.
 12.

554

4. Discussion

556 4.1 Drivers of Holocene land cover change in North America: scaling from taxon-level regional dynamics to continental-scale trends



558 These continental-scale Holocene changes in land cover (Figs. 2-3) are an emergent outcome of the
individualistic plant responses to deglaciation and multiple environmental changes, including seasonal
560 temperatures, effective moisture, atmospheric carbon dioxide, soil development, fire and other
disturbance regimes, and, at some locations during the late Holocene, human land use. As shown here
562 (Figs. 4-7), this interplay differed spatially across North America, often with opposing trends (e.g.
simultaneous increases in evergreen cover in some regions and decreases elsewhere) that partially offset
564 at the continental scale.

The first-order continental-scale drivers of Holocene land cover change in North America were
566 changing climates and the retreat and disappearance of the Laurentide Ice Sheet, particularly during the
early Holocene (11.7 to 7.5 ka) and lasting until 5.7 ka, with the disappearance of remnant ice in the
568 Labrador Dome in northern Quebec (Dalton et al., 2020). Deglaciation and an overall increase in land
availability explains why all land cover types show an increase in area-weighted cover during the early
570 Holocene, with evergreen taxa showing the greatest gain (Fig. 3). Continental temperatures also closely
tracked the decline in ice area (Marsicek et al., 2018), and vegetation responded to both factors.
572 Superimposed upon the early-Holocene increase in area-weighted cover for all PFTs are gains and losses
for each PFT at subregional scales (Figs. 4-7), which can be linked to climate-driven changes in plant
574 abundances at local to landscape scales that scaled upwards to continental-scale shifts in plant
distributions, with both within-range shifts in dominance and leading-edge and trailing-edge range
576 dynamics for individual plant taxa (Payette et al., 2022; Williams et al., 2004; George et al., 2023;
Dallmeyer et al., 2022; Anderson et al., 2017).

578 Leading-edge dynamics and range expansion of tree taxa appear to have been primarily
controlled by the increasing availability of deglaciated land area, end-Pleistocene warming, the declining
580 influence of ice sheet on regional climates and moisture availability (Alder and Hostetler, 2015; Bartlein
et al., 2014), and on-going expansion of plant taxa into areas of increased climate suitability (Payette et
582 al., 2022; Williams et al., 2004; George et al., 2023; Dallmeyer et al., 2022). Declining ice extent favored
moisture advection into eastern areas where most of the increase in summergreen tree taxa took place and
584 reduced it in midcontinental North America, where most of the open vegetation increase developed
(Shuman and Marsicek, 2016; Shuman et al., 2002; Liefert and Shuman, 2020). These changes in the
586 patterns of moisture availability simultaneously favored the large increase from 10 to 6 ka in
summergreen trees and shrubs in eastern North America south of the former Laurentide Ice Sheet and the
588 increase in open land in the mid-continent (Supplementary Fig. 2-3).

Declines in abundance and trailing-edge dynamics of tree taxa were likely governed by a
590 combination of declining climate suitability and, in some places, fire regimes, in which many local
populations failed to re-establish after one or more fire events. For example, in the high northern latitudes



592 of Quebec and Labrador, the expansion of open lands over the last three thousand years can be attributed
first to declining summer insolation and temperatures, caused by precessional changes in the Earth's orbit
594 (Payette, 2021), but at local to landscape and centennial scales, loss of forest cover was asynchronous and
caused by individual fire events (Payette et al., 2008; Gajewski et al., 2021). Similarly, in the southern
596 Great Lakes region and NEUS, the late-Pleistocene to early Holocene transition from conifer-dominated
forests and parklands to summergreen forests was driven by rising temperatures and changes in effective
598 moisture (Shuman et al., 2002; 2019), but accelerated locally by intensified fire regimes, with the timing
and rate of conversion varying among sites (Jensen et al., 2021; Clark et al., 1996). The expansion and
600 then retreat of the Great Plains prairies (Fig. 4) was driven by early Holocene aridification and middle-
to late-Holocene increases in moisture availability, while fire may have facilitated prairie expansion, but
602 delayed its retreat (Williams et al., 2009; Nelson et al., 2006; Umbanhower et al., 2006). Of course,
throughout North America, forests and fire dynamically co-existed and interacted during the Holocene
604 (Iglesias and Whitlock, 2020; Kelly et al., 2013), so whether fire causes transformative shifts in
ecosystem type depends on its synergistic interactions with directional changes in climate and other
606 factors (Napier and Chipman, 2021). Regardless of the role of fire or other disturbances, regional shifts in
temperature and moisture availability are usually the first-order predictors of Holocene changes in
608 vegetation composition (Dean et al., 1984; MacDonald, 1989; Calder and Shuman, 2017; Shuman et al.,
2004; Nelson et al., 2006).

610 The relative proportion of evergreen and summergreen cover types may have been affected by
changes in the length and intensity of the growing season during the Holocene, which is regulated by
612 precessional variations in insolation. In particular, the broad peak in summergreen tree cover between 8.5
and 3.5 ka (Fig. 3) is consistent with the hypothesis that summergreen tree and shrub abundances in North
614 America are partially regulated by summer insolation and temperatures (Delcourt and Delcourt, 1994;
Williams et al., 2001). Summer insolation reached higher peak intensity but has a shorter seasonal
616 duration in the early Holocene than during the late Holocene (Huybers, 2006; Jackson et al., 2009), which
may have favored plants with summer deciduous phenology that could more effectively exploit available
618 energy during a briefer but more intense growing season (Delcourt and Delcourt, 1994; Williams and
Jackson, 2007; Edwards et al., 2005). Indeed, pollen-reconstructed and CCSM3-simulated changes in
620 growing-degree days also peaked during the mid-Holocene when forest cover was greatest, and several
millennia after peak summer temperatures, likely because of differential responses of maximum summer
622 temperatures and total growing season warmth to orbital and other forcings (Marsicek et al., 2018). This
may in turn suggest a seasonal-scale feedback loop between summer insolation, deciduous phenology,
624 and total summer warmth (see Section 4.2).



626 During the late Holocene, human land use in the Americas intensified, with increasing effects
upon land cover and understanding the interactions among past climate change, fire regime, and human
land use is a highly active area of research. Rates of vegetation change worldwide began to increase
628 between 4.6 and 2.9 ka (Mottl et al., 2021), consistent with growing intensification and extent of land use
(Stephens et al., 2019). The 7 to 10 ppm decrease in global CO₂ between 1570 and 1620 CE has been
630 attributed to the land abandonment and reforestation due to mass mortality of Indigenous populations in
the Americas, caused by the spread of multiple pathogens (Lewis and Maslin, 2015). The best evidence
632 for dense human populations and extensive land clearance in the Americas comes from Central and
tropical South America (Islebe et al., 1996; McMichael, 2020).

634 In North America, the effects of human land use prior to EuroAmerican settlement are detectable
at some sites, but are not easily detected at the regional to continental scales addressed here. In North
636 America, the distribution of radiocarbon dates from archaeological contexts suggest that population levels
remained relatively low and increasing slowly until ~7 ka, with further increases between 7 and 2 ka, and
638 then rapidly increased after 2 ka (Peros et al., 2010). Indigenous cultures in North America clearly
engaged in activities that, in some areas, modified the composition and structures of forested and
640 unforested landscapes for millennia (Ellis, 2021; Delcourt et al., 1986; Leopold and Boyd, 1999; Munoz
et al., 2014). In densely populated regions, such as lands of the Iroquois Confederacy, southern Ontario,
642 or the Cherokee Nation, Cahokia and the American Riverbottom, land use altered vegetation structure and
composition at local to landscape scales, through management of fire regimes (Roos et al., 2018;
644 Anderson and Carpenter, 1991), land clearance for agricultural crops (McAndrews and Turton, 2007), and
silviculture, e.g. favoring the spread of nut-bearing trees (Munoz et al., 2014; Black et al., 2006). In
646 western North America, the effects of anthropogenic activity on vegetation and fire is an active area of
research, with several paleoecological studies indicating changes consistent with human influences on
648 forest composition (Walsh et al., 2015; Knight et al., 2022; Lacourse et al., 2007). Because the scale of
human action was strongest at local to landscape scales and varied in intensity within and among regions,
650 its detection often requires highly-focused, local- to regional-scale studies (Oswald et al., 2020; Roos,
2020; Lacourse et al., 2007; Knight et al., 2022; Munoz and Gajewski, 2010). These studies clearly
652 indicate a high intersite variance in the level and detectability of human impact. At the continental scale,
Gajewski et al. (2019) did not find clear correlations between human population abundance and pollen
654 abundance, including taxa of economic use or disturbance taxa, and concluded impacts were at local to
regional scales. Thus, at the regional to continental scales considered here, it is an open question whether
656 the rich relationships and diverse activities engaged by communities within their homelands led to
detectable changes in land cover types. We expect that pollen-based land cover reconstructions will



658 continue to contribute to interdisciplinary approaches to address anthropogenic fire and land cover change
during the Holocene (Snitker et al., 2022).

660 In contrast, after EuroAmerican arrival and expansion from 1492 onwards, North American
ecosystems were massively transformed (Stegner and Spanbauer, 2023) by multiple anthropogenic
662 processes. These include widespread forest conversion to agricultural and pastoral lands, intensive forest
harvesting, massive hydrological change through dam construction and wetland drainage, introduction of
664 exotic species and pests, and both greatly increased fire activity and fire suppression (Klein Goldewijk et
al., 2011; Foster and Aber, 2004).

666

4.2 Biophysical vegetation-atmosphere feedbacks to Holocene climates

4.1.1 Holocene vegetation-atmosphere feedbacks: prior work and need for data constraints

This paper and the other REVEALS-based reconstructions for the Northern Hemisphere (Githumbi et al.,
670 2022c; Li et al., 2020) are now laying the foundation for a next generation of Holocene vegetation-
atmosphere research with well-constrained land surface data. Many studies have explored the potential
672 impacts of vegetation-atmosphere feedbacks on Holocene climate dynamics at hemispheric to global
scales, but these studies have generally not employed well-constrained land cover reconstructions.
674 Treeline shifts have been recognized as an important regulator of Holocene vegetation-atmosphere
feedbacks in the high northern latitudes (TEMPO (Testing Earth System Models with Paleo-
676 Observations), 1996). Earth system model experiments with prescribed vegetation scenarios have shown
that, in the northern latitudes (45-90N), changes in forest cover are the largest contributor to changes in
678 net land surface radiation through snow masking and effects on surface albedo (Bathiany et al., 2010). In
mid-Holocene atmosphere-vegetation model simulations, strong snow masking resulted in warming three
680 times higher than those with weak snow masking (Otto et al., 2011). Additionally, empirical estimates of
surface-albedo feedbacks in high latitudes are stronger than predicted by climate models (Hogg, 2022).
682 More recent work has highlighted the importance of the type and density of forest cover in determining
the albedo feedback and magnitude of snow masking (Loranty et al., 2014; Alessandri et al., 2021).
684 Hence, because snow masking and surface albedo is an important regulator of surface-atmosphere
feedbacks in climate models, it is also an important source of uncertainty in Holocene climate
686 simulations, because of the limited availability of well-constrained reconstructions of past changes in
vegetation type, structure, and density. Vegetation structure and topographic complexity also jointly
688 govern surface roughness, which affects lower atmosphere temperature, humidity, wind speed, and soil
moisture (Bonan, 2015) and is the dominant land-cover influence on micrometeorological processes
690 (Chen and Dirmeyer, 2016). This new generation of LandCover6k vegetation reconstructions thus



692 promise to sharpen our understanding of the role played by surface-atmosphere feedbacks in Holocene
climate dynamics, with first results from Europe already underway (Strandberg et al., 2022b).

694 4.1.2 Assessing recent modeling studies of the Holocene conundrum

696 The Holocene Conundrum has been a major focus of paleoclimatic research over the last decade
(Kaufman and Broadman, 2023; Liu et al., 2014), and recent research has invoked vegetation-atmosphere
698 feedbacks to resolve this conundrum (Thompson et al., 2022). The Holocene Conundrum involves a
discrepancy between proxy-based reconstructions of global temperature changes, mostly based on marine
700 records, which indicate a mid-Holocene maximum and mid- to late-Holocene cooling (Marcott et al.,
2013), while transient model simulations show small but steady warming throughout the Holocene (Liu et
al., 2014). Many explanations for this discrepancy have since been proposed (Kaufman and Broadman,
702 2023). Recent prescribed-vegetation experiments in climate models produce an early Holocene warming
to a Holocene Thermal Maximum, followed by cooling towards the pre-industrial Holocene (Thompson
704 et al., 2022), consistent with paleoclimatic proxies. Conversely, experiments that include drivers such as
dust, ice cover, orbital forcing, and greenhouse gasses without accounting for Northern Hemisphere
706 vegetation changes do not result in a mid-Holocene thermal maximum (Thompson et al., 2022).

Our reconstructions suggest, however, that for North America, the prescribed vegetation maps
708 used by Thompson et al (2022) overstate the magnitude of Holocene vegetation change. These
prescribed-vegetation experiments for 9 and 6 ka fully replace all C₃ grasses with boreal forest for all
710 locations north of 50N (Thompson et al., 2022, Supp. Fig. 7B). This pattern is qualitatively consistent
with the early Holocene afforestation reported here (Fig. 2) but is inconsistent with the demonstrated
712 persistence of tundra throughout the early and middle Holocene, particularly in WCAN/AK (Figs. 2, 6)
and Canadian High Arctic (Fig. 2). Similarly, the prescribed full replacement of C₃ grasslands with
714 temperate deciduous forest for the 9 and 6 ka experiments (Thompson et al., 2022, Supp. Fig. 7B) is
inconsistent with clear palynological evidence of the establishment of the Great Plain grassland by the
716 early Holocene and prairie expansion during the early to middle Holocene (Fig. 2, Supp. Fig. 1) (Williams
et al., 2009a). Hence, the Thompson et al (2022) simulations should be viewed as useful experiments that
718 show the potential sensitivity of Holocene climates to large vegetation changes, but these experiments
likely overestimate the contribution of vegetation feedbacks to resolving the Holocene Conundrum.

720

4.1.3 Understudied Holocene vegetation-atmosphere feedbacks in North America

722 Our reconstructions also highlight several major features of North American vegetation dynamics
that may have underappreciated effects on Holocene vegetation-atmosphere feedbacks and climate
724 dynamics at regional to continental scales. First, the mid-Holocene decline and recovery of *Tsuga*



726 *canadensis* (eastern hemlock) in the northeastern United States is an example of how single-species
728 dynamics can drive fundamental changes in vegetational structure. Although the patterns and drivers of
730 the *T. canadensis* decline have been extensively studied (Oswald and Foster, 2012; Oswald et al., 2017;
732 Booth et al., 2012; Foster et al., 2006), the effects of the *T. canadensis* decline on Holocene climates are
734 unknown. As the dominant evergreen conifer of cool-temperate eastern North America, the decline of *T.*
736 *canadensis* at ca. 5 ka is the primary driver of the loss of ETS between 6 and 4 ka, while the gradual
recovery of *T. canadensis* after 5 ka drives the corresponding increase of ETS (Fig. 4). This shift in
dominance between summergreen and evergreen trees and shrubs, in turn, regulates the overall albedo of
the land surface and particularly its seasonal range. During times of foliage, summergreen forests can
have more than twice the albedo of evergreen forests (Hollinger et al., 2010). Summergreen forests also
exhibit much greater seasonal variability in albedo, with maximum values in full foliage being 20-50%
larger than annual lows.

Second, the peak in summergreen tree cover between ca. 8.5 and 4.5 ka (Fig. 2) may indicate a
seasonal-scale positive feedback loop between summer insolation, summergreen phenology, and summer
temperatures. Studies have suggested that the late-Pleistocene to early-Holocene peak in summer
insolation favored summergreen phenology and carbon acquisition strategies over evergreen strategies
(Delcourt and Delcourt, 1994; Williams and Jackson, 2007). Studies from the Pacific Northwest and
Alaska also show a peak in *Alnus* and other summergreen tree and shrub taxa during the early Holocene
(Fig. 7c), coincident with the summer insolation maximum and local maxima in temperature (Gavin et al.,
2013; Edwards et al., 2005; Whitlock, 1992). This climate-driven response, in turn, may have increased
the seasonal range of albedo and surface temperatures, thereby further favoring summergreen strategies.
This summergreen feedback might have also contributed to some summer cooling, due to the higher
summer albedo of summergreen trees (Hollinger et al., 2010). As an alternative hypothesis, Herzschuh,
(2020) suggested that the Eurasian distribution of evergreen spruce-dominated and deciduous larch-
dominated evergreen forests was due to historical contingencies and alternate stable states. Although
many studies have explored the effect of early to middle Holocene afforestation on vegetation feedbacks
in the northern latitudes (Brovkin et al., 2009; TEMPO (Testing Earth System Models with Paleo-
Observations), 1996), to our knowledge no paper has yet focused specifically on the seasonal feedback
effects associated with shifting proportions of summergreen and evergreen trees and shrubs.

754

4.3 Uncertainties and limitations in pollen-vegetation model reconstructions

756 Land cover reconstructions from pollen rely upon a variety of pollen-vegetation models (PVMs), some of
758 which have well-understood limitations and uncertainties, and some of which are newer and are still being
studied. The REVEALS PVM used here is has been widely adopted (e.g. Li et al., 2020; Githumbi et al.,



2022c; Serge et al., 2023; Azuara et al., 2019; Hoveers et al., 2022) because it represents some of the
760 taxon-level processes governing pollen production, transport, and representation (Sugita, 2007a; Prentice,
1985). However, processes such as atmospheric transport are simplified (Jackson and Lyford, 1999a) and
762 key parameters such as pollen productivity estimates (PPEs) carry uncertainties (Wieczorek and
Herzschuh, 2020; Broström et al., 2008; Hayashi et al., 2022) that translate to uncertainties in fractional-
764 weighted land cover area. Most PPE estimates are generated from models fitted to spatial networks of
vegetation surveys and surface pollen samples, and these PPE estimates depend strongly on models of
766 pollen dispersal (Theuerkauf et al., 2012).

Such issues may explain some of the surprising aspects of the reconstructions presented here. For
768 example, reconstructed *Acer* cover in the NEUS/SEC (Fig. 4c) is high compared to settlement-era
estimates from witness trees and land surveys (Thompson et al., 2013; Paciorek et al., 2016). Similarly,
770 reconstructed cover of *Abies* in both the NEUS/SEC and PCCS is higher than expected (Figs. 4c, 7c).
Abies and *Acer* are notoriously underrepresented in fossil pollen assemblages (Bradshaw and Webb,
772 1985), relative to independent surveys of tree abundance in the surrounding ecosystems, due to the low
pollen productivity of maple trees relative to other taxa (Finkelstein et al., 2006; Liu et al., 2022) and high
774 fall speeds of *Abies* (Jackson and Lyford, 1999b). Hence, a key value of process-based PVMs, such as
REVEALS, is the ability to correct for these known biases. However, REVEALS estimates are sensitive
776 to parameter choices and it is possible that the estimates of *Abies* and *Acer* are too high. There are few
estimates of *Abies* fall speeds compared to other taxa, and the fall speeds used here from Wieczorek and
778 Herzschuh (2020) are similar to the values for *Larix* that initial testing indicated led to *Larix*
overrepresentation.

780 REVEALS is not spatial or temporal in nature, so there is no representation of spatiotemporal
dependencies among site-level reconstructions. REVEALS estimates of uncertainty are based on the total
782 number of pollen grains counted in a sample and the error associated with the PPEs, but do not include
process uncertainty or uncertainty in other model inputs. The GMRF serves as a post-hoc interpolator to
784 generate spatio-temporally complete vegetation reconstructions, but this approach does not
mechanistically represent the underlying processes that link pollen to vegetation.

786 To address these limitations with the REVEALS workflow (spatio-temporal incompleteness,
input parameter uncertainty, and uncertainty quantification), other forms of PVMs have been developed.
788 ROPES uses pollen accumulation rates and REVEALS to estimate pollen productivity (Theuerkauf and
Couwenberg, 2018). However, the dependence of ROPES on pollen accumulation rates may limit its
790 widespread utility. At many sites, pollen accumulation rates have high uncertainties due to variations in
sedimentation rate, few radiometric dates and poor chronological controls, and spike counting
792 uncertainties (Perrotti et al., 2022). STEPPS is a Bayesian spatio-temporal PVM (Dawson et al., 2016,



2019b). While theoretically sound, STEPPS is computationally intensive and its estimates are dependent
794 upon the density and quality of spatial forest compositional calibration datasets, limiting its applicability
to regional-scale domains. Other spatial Bayesian models developed for high-resolution networks of
796 pollen and vegetation data suggest that if the spatial site density is too low, STEPPS and similarly
structured PVMs can over-estimate pollen dispersal distance (Liu et al., 2022).

798

4.4 Future work

800 With North American REVEALS-based reconstructions now in place, all middle- and high-latitudes in
the Northern Hemisphere have quantitative reconstructions of Holocene land cover that are well
802 constrained by dense networks of fossil pollen records (Githumbi et al., 2022a; Li et al., 2020). The
reconstructions for North America and Europe also have estimates of uncertainty from the spatiotemporal
804 GMRF model (Pirzamanbein et al., 2018a). This hemispheric coverage now enables the creation of a
next generation of modeling scenarios, well-constrained by data, to explore land cover feedbacks in the
806 Holocene climate system (Harrison et al., 2020). These land cover reconstructions also help identify
places where new local-scale, site-based research are needed to better understand human impacts, better
808 constrain land cover changes in areas of sparse data and high uncertainty, and better understand how local
and taxon-level dynamics scale up to affect regional- to continental-scale vegetation and climate
810 dynamics.

This work also underscores the critical need for more work to better constrain PPEs and fall
812 speeds, particularly for North American plant taxa. The REVEALS estimates in this analysis appear to be
particularly sensitive to the parameterizations for underrepresented taxa such as *Abies* and *Acer*.

814 Lastly, given the maturation of pollen-vegetation modeling as a field of study and the emergence
of multiple PVMs, there is now the opportunity for intercomparison studies among PVMs and, perhaps,
816 the development of ensemble-based inferences of past vegetation cover. There is a long history of
methodological comparisons in pollen-based paleoclimatic inferences and paleoclimatology more broadly
818 (Chevalier et al., 2020). Few systematic intercomparisons of PVMs yet exist (Roberts et al., 2018),
although individual papers have discussed strengths and weaknesses of different modeling approaches
820 (Liu et al., 2022; Theuerkauf et al., 2012). Initial efforts are underway to compare land cover
reconstructions from REVEALS-GMRF to those from the Bayesian spatio-temporal model STEPPS.
822 Moreover, given that ensemble-based approaches have been shown to have higher predictive ability in
fields such as climate modeling and species distribution modeling (Deser et al., 2020; Bothe et al., 2013;
824 Rangel et al., 2009; Thuiller et al., 2009), there is value in developing approaches for ensemble-based
PVMs for past land cover inference.



826 5. Conclusions

827 Continental-scale changes in land cover in North America during the Holocene are the outcome of
828 multiple interacting drivers operating over a range of temporal and spatial scales. For much of the
829 Holocene (ca. 8 to 1.5 ka), the spatial configurations of continental-scale fractional forest cover were
830 broadly stable. Major continental-scale trends included early Holocene afforestation, a middle-Holocene
831 peak in the areal proportion of summergreen trees and shrubs, and a last-millennium increase in open
832 land. These trends were powered by taxon-level dynamics that varied within and among regions. The
833 regional dynamics can be attributed to individualistic postglacial shifts in the range and abundance of
834 plant taxa driven by changing climates and increased land area after deglaciation; abrupt and large
835 species-level events, such as the mid-Holocene collapse of eastern hemlock; and a shift from localized
836 land use during the late Holocene to massive ecosystem transformation following EuroAmerican
837 settlement. This work rejects the ideas of both pre-industrial forest stability and widespread major
838 conversions in land cover type.

839 This work contributes to the LandCover6k initiative to produce continental- to global-scale
840 reconstructions of Holocene land cover dynamics that are well-constrained by proxy data and are
841 quantified using consistent methods. These REVEALS-GMRF reconstructions can help refine Holocene
842 models of land use and land cover change, provide a foundation for comparisons among PVMs, indicate
843 priority areas for future new site-level research, and establish realistic benchmark scenarios constraining
844 and assimilating with Earth system model simulations of the interactions among Holocene climate, land
845 cover, and anthropogenic change. Scaling up from these continental to hemispheric and global products
846 will enable further testing of hypotheses about the drivers and feedbacks of Holocene land cover change.
847 These reconstructions also highlight several potentially important but unstudied vegetation-atmosphere
848 feedbacks, including the collapse of eastern hemlock at ca. 5 ka and a positive feedback loop between
849 mid-Holocene peaks in seasonality of insolation, temperature, and vegetation phenology.

850 Comparison of the REVEALS-GMRF land cover reconstructions with those inferred from
851 alternate PVMs is a research priority. REVEALS-GMRF depends on a suite of input variables that are
852 both uncertain and exhibit spatial and temporal variation not accounted for in the model. Also, the use of
853 a post-hoc Bayesian GMRF interpolation step means that uncertainty of reconstructions associated with
854 these assumptions is not fully characterized.

855 Finally, this work emphasizes the importance of quantifying ecosystem processes and feedbacks
856 between the land surface and climate system. Holocene land cover changes in North America are non-
857 negligible and there is a pressing need to refine ecosystem models, in particular when those models are
858 coupled within an Earth System model. The availability of well-constrained data products has been a



major barrier to this effort. Paleocology and palynology are reaching a new level of maturity with
860 respect to advances in data discovery and accessibility, as well as development of consistent analytical
methods that permit interpretability of large-scale spatio-temporal change. Data assimilation experiments
862 that integrate these reconstructions into Earth System models have the potential to resolve major
questions in the field, such as the Holocene Conundrum and disentangling the effects of climate-
864 vegetation-human interactions upon Holocene vegetation and climate dynamics.

6. Code and data availability

866 Code and data used in this workflow are publicly available at <https://github.com/andydawson/reveals-na>.
The REVEALS-GMRF reconstructions are available at
868 https://github.com/BehnazP/SpatioCompo_entireHolocene_NA. The description and implementation of the
digitization of lake area is available at https://github.com/NeotomaDB/neotoma_lakes.

870 7. Author contributions

AD and JWW co-designed and co-wrote the paper, with AD leading on REVEALS analyses and figure
872 generation. MJG helped initiate this effort, led PAGES LandCover6k, and coordinated activities with
other continental-scale mapping groups. BP and JL assisted with the GMRF modeling and analyses,
874 while SG assisted with Neotoma data provision and digitization of lake size. RSA, AB, DF, KG, DG, TL,
TM, WO, BS, and CW all contributed new records to the North American Pollen Database in Neotoma
876 and assisted in data interpretation. All authors contributed to manuscript development and revision.

8. Competing interests

878 The authors declare that they have no conflict of interest.

9. Acknowledgments

880 This work is a contribution to the Past Global Change (PAGES) project and its working group
LandCover6k (<https://pastglobalchanges.org/science/wg/former/landcover6k/intro>), which in turn
882 received support from the Swiss National Science Foundation, the Swiss Academy of Sciences, the US
National Science Foundation, and the Chinese Academy of Sciences. This work is also supported
884 through an NSERC Discovery Grant to A. Dawson. M.-J. Gaillard received support from the Swedish
Strategic Research Area (SRA) MERGE (Modelling the Regional and Global Earth system;



886 <http://www.merge.lu.se>. Data were obtained from the Neotoma Paleoecology Database
888 (<http://www.neotomadb.org>) and its constituent database the North American Pollen Database. The work
889 of data contributors, data stewards, and the Neotoma community is gratefully acknowledged. Support for
Neotoma is from the NSF-Geoinformatics program (1948926). Digitization of basin areas was assisted
890 by Jenna Kilsevich, Grace Roper, Claire Rubbelke, Grace Tunski, Mathias Trachsel, and Bailey Zak.



892 10. References

- 894 Abraham, V., Oušková, V., and Kuneš, P.: Present-day vegetation helps quantifying past land cover in selected regions of the Czech Republic, *PLoS One*, 9, e100117, 2014.
- 896 Alder, J. R. and Hostetler, S. W.: Global climate simulations at 3000-year intervals for the last 21 000 years with the GENMOM coupled atmosphere–ocean model, *Clim. Past*, 11, 449–471, <https://doi.org/10.5194/cp-11-449-2015>, 2015.
- 898 Alessandri, A., Catalano, F., De Felice, M., Van den Hurk, B., and Balsamo, G.: Varying snow and vegetation signatures of surface-albedo feedback on the Northern Hemisphere land warming, *Environ. Res. Lett.*, 16, 034023, 2021.
- 902 Allison, T. D., Moeller, R. E., and Davis, M. B.: Pollen in laminated sediments provides evidence of mid-Holocene forest pathogen outbreak, *Ecology*, 67, 1101–1105, 1986.
- 904 Alt, M., McWethy, D. B., Everett, R., and Whitlock, C.: Millennial scale climate-fire-vegetation interactions in a mid-elevation mixed coniferous forest, Mission Range, northwestern Montana, USA, *Quat. Res.*, 90, 66–82, 2018.
- 906 Anderson, L. L., Hu, F. S., Nelson, D. M., Petit, R. J., and Paige, K. N.: Ice-age endurance: DNA evidence of a white spruce refugium in Alaska, *Proc. Natl. Acad. Sci.*, 103, 12447–12450, 2006.
- 908 Anderson, P. M. and Brubaker, L. B.: Vegetation history of northcentral Alaska: A mapped summary of late-Quaternary pollen data, *Quat. Sci. Rev.*, 13, 71–92, [https://doi.org/10.1016/0277-3791\(94\)90125-2](https://doi.org/10.1016/0277-3791(94)90125-2), 1994.
- 912 Anderson, R. S.: Postglacial biogeography of Sierra lodgepole pine (*Pinus contorta* var. *murrayana*) in California, *Écoscience*, 3, 343–351, <https://doi.org/10.1080/11956860.1996.11682352>, 1996.
- 914 Anderson, R. S. and Carpenter, S. L.: Vegetation change in Yosemite Valley, Yosemite National Park, California, during the protohistoric period, *Madroño*, 38, 1–13, 1991.
- 916 Anderson, R. S., Davis, R. B., Miller, N. G., and Stuckenrath, Jr., R.: History of late- and post-glacial vegetation and disturbance around Upper South Branch Pond, northern Maine, *Can. J. Bot.*, 64, 1977–1986, 1986.
- 918 Anderson, R. S., Allen, C. D., Toney, J. L., Jass, R. B., and Bair, A. N.: Holocene vegetation and fire regimes in subalpine and mixed conifer forests, southern Rocky Mountains, USA, *Int. J. Wildland Fire*, 17, 96–114, 2008.
- 922 Anderson, R. S., Kaufman, D. S., Berg, E., Schiff, C., and Daigle, T.: Holocene biogeography of *Tsuga mertensiana* and other conifers in the Kenai Mountains and Prince William Sound, south-central Alaska, *The Holocene*, 27, 485–495, <https://doi.org/10.1177/0959683616670217>, 2017.
- 924 Anderson, R. S., Berg, E., Williams, C., and Clark, T.: Postglacial vegetation community change over an elevational gradient on the western Kenai Peninsula, Alaska: pollen records from Sunken Island and Choquette Lakes, *J. Quat. Sci.*, 34, 309–322, <https://doi.org/10.1002/jqs.3102>, 2019.
- 926



- 928 Azuara, J., Mazier, F., Lebreton, V., Sugita, S., Viovy, N., and Combourieu-Nebout, N.: Extending the applicability of the REVEALS model for pollen-based vegetation reconstructions to coastal lagoons, *The Holocene*, 29, 1109–1112, 2019.
- 930 Bartlein, P. J., Hostletler, S. W., and Alder, J. R.: Paleoclimate, in: *Climate Change in North America*, Springer International Publishing, 1–51, 2014.
- 932 Bathiany, S., Claussen, M., Brovkin, V., Raddatz, T., and Gayler, V.: Combined biogeophysical and biogeochemical effects of large-scale forest cover changes in the MPI earth system model,
934 *Biogeosciences*, 7, 1383–1399, 2010.
- 936 Bhiry, N. and Filion, L.: Mid-Holocene hemlock decline in eastern North America linked with phytophagous insect activity, *Quat. Res.*, 45, 312–320, 1996.
- 938 Black, B. A., Ruffner, C. M., and Abrams, M. D.: Native American influences on the forest composition of the Allegheny Plateau, northwest Pennsylvania, *Can. J. For. Res.*, 36, 1266–1275, <https://doi.org/10.1139/x06-027>, 2006.
- 940 Bodmer, H.: Über den windpollen, *Nat. Tech.*, 3, 294–298, 1922.
- Bonan, G.: *Ecological climatology: concepts and applications*, 2015.
- 942 Bonan, G. B. and Doney, S. C.: Climate, ecosystems, and planetary futures: The challenge to predict life in Earth system models, *Science*, 359, eaam8328, 2018.
- 944 Booth, R. K., Brewer, S., Blaauw, M., Minckley, T. A., and Jackson, S. T.: Decomposing the mid-Holocene *Tsuga* decline in eastern North America, *Ecology*, 93, 1841–1852, <https://doi.org/10.1890/11-2062.1>, 2012.
- 948 Bothe, O., Jungclaus, J. H., Zanchettin, D., and Zorita, E.: Climate of the last millennium: ensemble consistency of simulations and reconstructions, *Clim Past*, 9, 1089–1110, <https://doi.org/10.5194/cp-9-1089-2013>, 2013.
- 950 Bradshaw, R. H. W. and Webb, I., T.: Relationships between contemporary pollen and vegetation data from Wisconsin and Michigan, USA, *Ecology*, 66, 721–737, 1985.
- 952 Briles, C. E., Whitlock, C., Bartlein, P. J., and Higuera, P.: Regional and local controls on postglacial vegetation and fire in the Siskiyou Mountains, northern California, USA, *Palaeogeogr. Palaeoclimatol. Palaeoecol.*, 265, 159–169, 2008.
- 956 Broström, A., Nielsen, A. B., Gaillard, M.-J., Hjelle, K., Mazier, F., Binney, H., Bunting, J., Fyfe, R., Meltsov, V., and Poska, A.: Pollen productivity estimates of key European plant taxa for quantitative reconstruction of past vegetation: a review, *Veg. Hist. Archaeobotany*, 17, 461–478, 2008.
- 958 Brovkin, V., Raddatz, T., Reick, C. H., Claussen, M., and Gayler, V.: Global biogeophysical interactions between forest and climate, *Geophys. Res. Lett.*, 36, 2009.
- 960 Brugam, R. B. and Swain, P.: Diatom indicators of peatland development at Pogonia Bog Pond, Minnesota, USA, *The Holocene*, 10, 453–464, <https://doi.org/10.1191/095968300668251084>, 2000.



- 962 Brugger, S. O. and Rhode, D.: Impact of Pleistocene–Holocene climate shifts on vegetation and fire
964 dynamics and its implications for Prearchaic humans in the central Great Basin, USA, *J. Quat. Sci.*, 35,
987–993, <https://doi.org/10.1002/jqs.3248>, 2020.
- 966 Calder, W. J. and Shuman, B. N.: Extensive wildfires, climate change, and an abrupt state change in
subalpine ribbon forests, Colorado, *Ecology*, 98, 2585–2600, 2017.
- 968 Chandan, D. and Peltier, W. R.: African Humid Period Precipitation Sustained by Robust Vegetation,
Soil, and Lake Feedbacks, *Geophys. Res. Lett.*, 47, e2020GL088728,
<https://doi.org/10.1029/2020GL088728>, 2020.
- 970 Chaput, M. A. and Gajewski, K.: Relative pollen productivity estimates and changes in Holocene
972 vegetation cover in the deciduous forest of southeastern Quebec, Canada, *Botany*, 96, 299–317,
<https://doi.org/10.1139/cjb-2017-0193>, 2018.
- 974 Chen, J., Zhang, Q., Huang, W., Lu, Z., Zhang, Z., and Chen, F.: Northwestward shift of the northern
976 boundary of the East Asian summer monsoon during the mid-Holocene caused by orbital forcing and
vegetation feedbacks, *Quat. Sci. Rev.*, 268, 107136, <https://doi.org/10.1016/j.quascirev.2021.107136>,
2021.
- 978 Chen, L. and Dirmeyer, P. A.: Adapting observationally based metrics of biogeophysical feedbacks from
land cover/land use change to climate modeling, *Environ. Res. Lett.*, 11, 034002, 2016.
- 980 Chevalier, M., Davis, B. A. S., Heiri, O., Seppä, H., Chase, B. M., Gajewski, K., Lacourse, T., Telford, R.
J., Finsinger, W., Guiot, J., Kühl, N., Maezumi, S. Y., Tipton, J. R., Carter, V. A., Brussel, T., Phelps, L.
982 N., Dawson, A., Zanon, M., Vallé, F., Nolan, C., Mauri, A., de Vernal, A., Izumi, K., Holmström, L.,
Marsicek, J., Goring, S., Sommer, P. S., Chaput, M., and Kupriyanov, D.: Pollen-based climate
984 reconstruction techniques for late Quaternary studies, *Earth-Sci. Rev.*, 210, 103384,
<https://doi.org/10.1016/j.earscirev.2020.103384>, 2020.
- 986 Clark, J. S., Hussey, T., and Royall, P. D.: Presettlement analogs for Quaternary fire regimes in eastern
North America, *J. Paleolimnol.*, 16, 79–96, 1996.
- 988 Cruz-Silva, E., Harrison, S. P., Marinova, E., and Prentice, I. C.: A new method based on surface-sample
pollen data for reconstructing palaeovegetation patterns, *J. Biogeogr.*, 49, 1381–1396,
<https://doi.org/10.1111/jbi.14448>, 2022.
- 990 Cwynar, L. C. and Spear, R. W.: Paleovegetation and paleoclimatic changes in the Yukon at 6 ka BP,
Géographie Phys. Quat., 49, 29–35, 1995.
- 992 Dallmeyer, A., Kleinen, T., Claussen, M., Weitzel, N., Cao, X., and Herzschuh, U.: The deglacial forest
conundrum, *Nat. Commun.*, 13, 6035, <https://doi.org/10.1038/s41467-022-33646-6>, 2022.
- 994 Dallmeyer, A., Poska, A., Marquer, L., Seim, A., and Gaillard-Lemdahl, M.-J.: The challenge of
996 comparing pollen-based quantitative vegetation reconstructions with outputs from vegetation models—a
European perspective, *Clim. Past Discuss.*, 2023, 1–50, 2023.
- 998 Dalton, A. S., Margold, M., Stokes, C. R., Tarasov, L., Dyke, A. S., Adams, R. S., Allard, S., Arends, H.
E., Atkinson, N., Attig, J. W., Barnett, P. J., Barnett, R. L., Batterson, M., Bernatchez, P., Borns, H. W.,
Breckenridge, A., Briner, J. P., Brouard, E., Campbell, J. E., Carlson, A. E., Clague, J. J., Curry, B. B.,
1000 Daigneault, R.-A., Dubé-Loubert, H., Easterbrook, D. J., Franzi, D. A., Friedrich, H. G., Funder, S.,



- 1002 Gauthier, M. S., Gowan, A. S., Harris, K. L., Hétu, B., Hooyer, T. S., Jennings, C. E., Johnson, M. D.,
Kehew, A. E., Kelley, S. E., Kerr, D., King, E. L., Kjeldsen, K. K., Knaeble, A. R., Lajeunesse, P.,
1004 Lakeman, T. R., Lamothe, M., Larson, P., Lavoie, M., Loope, H. M., Lowell, T. V., Lusardi, B. A., Manz,
L., McMartin, I., Nixon, F. C., Occhietti, S., Parkhill, M. A., Piper, D. J. W., Pronk, A. G., Richard, P. J.
1006 H., Ridge, J. C., Ross, M., Roy, M., Seaman, A., Shaw, J., Stea, R. R., Teller, J. T., Thompson, W. B.,
Thorleifson, L. H., Utting, D. J., Veillette, J. J., Ward, B. C., Weddle, T. K., and Wright, H. E.: An
1008 updated radiocarbon-based ice margin chronology for the last deglaciation of the North American Ice
Sheet Complex, *Quat. Sci. Rev.*, 234, 106223, <https://doi.org/10.1016/j.quascirev.2020.106223>, 2020.
- 1010 Davis, M. B.: Pollen evidence of changing land use around the shores of Lake Washington, *Northwest
Sci.*, 47, 133–148, 1973.
- 1012 Davis, M. B.: Outbreaks of forest pathogens in Quaternary history, in: *Proceedings of the Fourth
International Palynological Conference*, Lucknow, India, 216–227, 1981.
- 1014 Davis, M. B.: Palynology after Y2K—understanding the source area of pollen in sediments, *Annu. Rev.
Earth Planet. Sci.*, 28, 1–18, 2000.
- 1016 Dawson, A., Paciorek, C. J., McLachlan, J. S., Goring, S., Williams, J. W., and Jackson, S. T.:
Quantifying pollen-vegetation relationships to reconstruct ancient forests using 19th-century forest
composition and pollen data, *Quat. Sci. Rev.*, 137, 156–175, 2016.
- 1018 Dawson, A., Cao, X., Chaput, M., Hopla, E., Li, F., Edwards, M., Fyfe, R., Gajewski, K., Goring, S.,
Herzschuh, U., and others: Finding the magnitude of human-induced Northern Hemisphere land-cover
1020 transformation between 6 and 0.2 ka BP, *PAGES Mag.*, 26, 34–35, 2018.
- 1022 Dawson, A., Paciorek, C. J., Goring, S. J., Jackson, S. T., McLachlan, J. S., and Williams, J. W.:
Quantifying trends and uncertainty in prehistoric forest composition in the upper Midwestern United
States, *Ecology*, 100, e02856, <https://doi.org/10.1002/ecy.2856>, 2019a.
- 1024 Dawson, A., Paciorek, C. J., Goring, S., Jackson, S., McLachlan, J., and Williams, J. W.: Quantifying
trends and uncertainty in prehistoric forest composition in the upper Midwestern United States, *Ecology*,
1026 doi: 10.1002/ecy.2856, 2019b.
- 1028 Dean, W. E., Bradbury, J. P., Anderson, R. Y., and Barnosky, C. W.: The variability of Holocene climate
change: Evidence from varved lake sediments, *Science*, 226, 1191–1194,
<https://doi.org/10.1126/science.226.4679.1191>, 1984.
- 1030 Delcourt, H. R. and Delcourt, P. A.: Postglacial rise and decline of *Ostrya virginiana* (Mill) K Koch and
1032 *Carpinus caroliniana* Walt in eastern North-America: Predictable responses of forest species to cyclic
changes in seasonality of climates, *J. Biogeogr.*, 21, 137–150, 1994.
- 1034 Delcourt, P. A., Delcourt, H. R., Cridlebaugh, P. A., and Chapman, J.: Holocene ethnobotanical and
paleoecological record of human impact on vegetation in the Little Tennessee River Valley, Tennessee,
Quat. Res., 25, 330–349, 1986.
- 1036 Deser, C., Lehner, F., Rodgers, K. B., Ault, T., Delworth, T. L., DiNezio, P. N., Fiore, A., Frankignoul,
C., Fyfe, J. C., Horton, D. E., Kay, J. E., Knutti, R., Lovenduski, N. S., Marotzke, J., McKinnon, K. A.,
1038 Minobe, S., Randerson, J., Screen, J. A., Simpson, I. R., and Ting, M.: Insights from Earth system model
initial-condition large ensembles and future prospects, *Nat. Clim. Change*, 10, 277–286,
1040 <https://doi.org/10.1038/s41558-020-0731-2>, 2020.



- 1042 Edwards, M. E., Brubaker, L. B., Lozhkin, A. V., and Anderson, P. M.: Structurally novel biomes: a response to past warming in Beringia, *Ecology*, 86, 1696–1703, 2005.
- 1044 Ellis, E. C.: Land use and ecological change: A 12,000-Year History, *Annu. Rev. Environ. Resour.*, 46, 1–33, <https://doi.org/10.1146/annurev-environ-012220-010822>, 2021.
- 1046 Evans, M. N., Tolwinski-Ward, S. E., Thompson, D. M., and Anchukaitis, K. J.: Applications of proxy system modeling in high resolution paleoclimatology, *Quat. Sci. Rev.*, 76, 16–28, <http://dx.doi.org/10.1016/j.quascirev.2013.05.024>, 2013.
- 1048 Faison, E. K., Foster, D. R., Oswald, W. W., Hansen, B. C. S., and Doughty, E.: Early Holocene openlands in southern New England, *Ecology*, 87, 2537–2547, 2006.
- 1050 Finkelstein, S. A., Gajewski, K., and Viau, A. E.: Improved resolution of pollen taxonomy allows better biogeographical interpretation of post-glacial forest development: analyses from the North American Pollen Database, *J. Ecol.*, 94, 415–430, 2006.
- 1054 Flantua, S. G. A., Mottl, O., Felde, V. A., Bhatta, K. P., Birks, H. H., Grytnes, J.-A., Seddon, A. W. R., and Birks, H. J. B.: A guide to the processing and standardization of global palaeoecological data for large-scale syntheses using fossil pollen, *Glob. Ecol. Biogeogr.*, n/a, <https://doi.org/10.1111/geb.13693>, 2023.
- 1056
- 1058 Foley, J. A., Kutzbach, J. E., Coe, M. T., and Levis, S.: Feedbacks between climate and boreal forests during the Holocene epoch, *Nature*, 371, 52–54, 1994.
- 1060 Foster, D. R. and Aber, J. D.: *Forests in Time: The Environmental Consequences of 1000 Years of Change in New England*, Yale University Press, New Haven, CT., 2004.
- 1062 Foster, D. R., Oswald, W. W., Faison, E. K., Doughty, E. D., and Hansen, B. C. S.: A climatic driver for abrupt mid-Holocene vegetation dynamics and the hemlock decline in New England, *Ecology*, 87, 2959–2966, 2006.
- 1064 Fréchette, B., Richard, P. J. H., Grondin, P., Lavoie, M., and Larouche, A. C.: Postglacial history of the vegetation and climate of the spruce and fir forests of western Quebec, *Mém. Rech. For.*, 179, 2018.
- 1066 Fréchette, B., Richard, P. J. H., Lavoie, M., Grondin, P., and Larouche, A. C.: Histoire postglaciaire de la végétation et du climat des pessières et des sapinières de l’est du Québec et du Labrador méridional, *Mém. Rech. For.*, 186, 170, 2021.
- 1068
- 1070 Fyfe, R., Roberts, N., and Woodbridge, J.: A pollen-based pseudobiomisation approach to anthropogenic land-cover change, *The Holocene*, 20, 1165–1171, <https://doi.org/10.1177/0959683610369509>, 2010.
- 1072 Gaillard, M., Whitehouse, N., Madella, M., Morrison, K., and von Gunten, L.: Past Land Use and Land Cover., *PAGES Mag.*, 26, 2018.
- 1074 Gaillard, M. J. and Group, L. I. S.: LandCover6k: Global anthropogenic land-cover change and its role in past climate, *PAGES Mag.*, 23, 38–39, 2015.
- 1076 Gaillard, M.-J., Sugita, S., Mazier, F., Trondman, A.-K., Broström, A., Hickler, T., Kaplan, J. O., Kjellström, E., Kokfelt, U., Kuneš, P., Lemmen, C., Miller, P., Olofsson, J., Poska, A., Rundgren, M., Smith, B., Strandberg, G., Fyfe, R., Nielsen, A. B., Alenius, T., Balakauskas, L., Barnekow, L., Birks, H.



- 1078 J. B., Bjune, A., Björkman, L., Giesecke, T., Hjelle, K., Kalnina, L., Kangur, M., van der Knaap, W. O.,
1080 Koff, T., Lagerås, P., Latalowa, M., Leydet, M., Lechterbeck, J., Lindbladh, M., Odgaard, B., Peglar, S.,
Segerström, U., von Stedingk, H., and Seppä, H.: Holocene land-cover reconstructions for studies on land
cover-climate feedbacks, *Clim. Past*, 6, 483–499, <https://doi.org/10.5194/cp-6-483-2010>, 2010.
- 1082 Gajewski, K.: Environmental history of the northwestern Québec Treeline, *Quat. Sci. Rev.*, 206, 29–43,
<https://doi.org/10.1016/j.quascirev.2018.12.025>, 2019.
- 1084 Gajewski, K., Kriesche, B., Chaput, M. A., Kulik, R., and Schmidt, V.: Human–vegetation interactions
during the Holocene in North America, *Veg. Hist. Archaeobotany*, 28, 635–647,
1086 <https://doi.org/10.1007/s00334-019-00721-w>, 2019.
- Gajewski, K., Grenier, A., and Payette, S.: Climate, fire and vegetation history at treeline east of Hudson
1088 Bay, northern Québec, *Quat. Sci. Rev.*, 254, 106794, <https://doi.org/10.1016/j.quascirev.2021.106794>,
2021.
- 1090 Gavin, D. G. and Brubaker, L. B.: Late Pleistocene and Holocene Environmental Change on the Olympic
Peninsula, Washington, Springer, 2014.
- 1092 Gavin, D. G., Brubaker, L. B., and Greenwald, D. N.: Postglacial climate and fire-mediated vegetation
change on the western Olympic Peninsula, Washington (USA), *Ecol. Monogr.*, 83, 471–489,
1094 <https://doi.org/10.1890/12-1742.1>, 2013.
- Gavin, D. G., White, A., Sanborn, P. T., and Hebda, R. J.: Deglacial landforms and Holocene vegetation
1096 trajectories in the northern interior cedar-hemlock forests of British Columbia, in: *Untangling the
Quaternary Period—A Legacy of Stephen C. Porter*, vol. 548, edited by: Waitt, R. B., Thackray, G. D.,
1098 and Gillespie, A. R., Geological Society of America, 0, [https://doi.org/10.1130/2020.2548\(05\)](https://doi.org/10.1130/2020.2548(05)), 2021.
- George, A., Widell, S., Goring, S. J., Roth, R. E., and Williams, J. W.: Range Mapper: An adaptable
1100 process for making and using interactive, animated web maps of late-Quaternary open paleoecological
data, *Open Quat.*, 9, 15, <https://doi.org/10.5334/oq.114>, 2023.
- 1102 Githumbi, E., Fyfe, R., Gaillard, M.-J., Trondman, A.-K., Mazier, F., Nielsen, A.-B., Poska, A., Sugita,
S., Woodbridge, J., Azuara, J., Feurdean, A., Grindean, R., Lebreton, V., Marquer, L., Nebout-
1104 Combourieu, N., Stančikaitė, M., Tanțău, I., Tonkov, S., Shumilovskikh, L., and LandClimII data
contributors: European pollen-based REVEALS land-cover reconstructions for the Holocene:
1106 methodology, mapping and potentials, *Earth Syst Sci Data*, 14, 1581–1619, <https://doi.org/10.5194/essd-14-1581-2022>, 2022a.
- 1108 Githumbi, E., Pirzamanbein, B., Lindström, J., Poska, A., Fyfe, R., Mazier, F., Nielsen, A. B., Sugita, S.,
Trondman, A.-K., Woodbridge, J., and Gaillard, M.-J.: Pollen-Based Maps of Past Regional Vegetation
1110 Cover in Europe Over 12 Millennia—Evaluation and Potential, *Front. Ecol. Evol.*, 10,
<https://doi.org/10.3389/fevo.2022.795794>, 2022b.
- 1112 Githumbi, E., Pirzamanbein, B., Lindström, J., Poska, A., Fyfe, R., Mazier, F., Nielsen, A. B., Sugita, S.,
Trondman, A.-K., Woodbridge, J., and others: Pollen-Based Maps of Past Regional Vegetation Cover in
1114 Europe Over 12 Millennia—Evaluation and Potential, *Front. Ecol. Evol.*, 10, 795794, 2022c.
- Giuliano, C. and Lacourse, T.: Holocene fire regimes, fire-related plant functional types, and climate in
1116 south-coastal British Columbia forests, *Ecosphere*, 14, e4416, <https://doi.org/10.1002/ecs2.4416>, 2023.



- Goring, S.: neotoma_lakes, 2021.
- 1118 Grimm, E. C., Keltner, J., Cheddadi, R., Hicks, S., Lézine, A.-M., Berrio, J. C., and Williams, J. W.:
1120 Pollen databases and their application, in: Encyclopedia of Quaternary Science, edited by: Elias, S. A. and
Mock, C. J., Elsevier, 831–838, 2013.
- 1122 Gugger, P. F. and Sugita, S.: Glacial populations and postglacial migration of Douglas-fir based on fossil
pollen and macrofossil evidence, *Quat. Sci. Rev.*, 29, 2052–2070, 2010.
- 1124 Haas, J. N. and McAndrews, J. H.: The summer drought related hemlock (*Tsuga canadensis*) decline in
eastern North America 5,700 to 5,100 years ago, Symposium on Sustainable Management of Hemlock
Ecosystems in Eastern North America, 1999.
- 1126 Hansen, B. C. S. and Engstrom, D. R.: Vegetation History of Pleasant Island, Southeastern Alaska, since
13,000 yr B.P., *Quat. Res.*, 46, 161–175, <https://doi.org/10.1006/qres.1996.0056>, 1996.
- 1128 Harrison, S. P., Gaillard, M. J., Stocker, B. D., Vander Linden, M., Klein Goldewijk, K., Boles, O.,
1130 Braconnot, P., Dawson, A., Fluet-Chouinard, E., Kaplan, J. O., Kastner, T., Pausata, F. S. R., Robinson,
E., Whitehouse, N. J., Madella, M., and Morrison, K. D.: Development and testing scenarios for
1132 implementing land use and land cover changes during the Holocene in Earth system model experiments,
Geosci Model Dev, 13, 805–824, <https://doi.org/10.5194/gmd-13-805-2020>, 2020.
- 1134 Hayashi, R., Sasaki, N., Takahara, H., Sugita, S., and Saito, H.: Estimation of absolute pollen productivity
based on the flower counting approach: A review, *Quat. Int.*, 641, 122–137, 2022.
- 1136 Hellman, S., Gaillard, M.-J., Broström, A., and Sugita, S.: The REVEALS model, a new tool to estimate
past regional plant abundance from pollen data in large lakes: validation in southern Sweden, *J. Quat. Sci.*
Publ. Quat. Res. Assoc., 23, 21–42, 2008a.
- 1138 Hellman, S. E., Gaillard, M., Broström, A., and Sugita, S.: Effects of the sampling design and selection of
1140 parameter values on pollen-based quantitative reconstructions of regional vegetation: a case study in
southern Sweden using the REVEALS model, *Veg. Hist. Archaeobotany*, 17, 445–459, 2008b.
- 1142 Herzschuh, U.: Legacy of the Last Glacial on the present-day distribution of deciduous versus evergreen
boreal forests, *Glob. Ecol. Biogeogr.*, 29, 198–206, <https://doi.org/10.1111/geb.13018>, 2020.
- 1144 Herzschuh, U., Böhmer, T., Li, C., Chevalier, M., Hébert, R., Dallmeyer, A., Cao, X., Bigelow, N. H.,
Nazarova, L., and Novenko, E. Y.: LegacyClimate 1.0: a dataset of pollen-based climate reconstructions
1146 from 2594 Northern Hemisphere sites covering the last 30 kyr and beyond, *Earth Syst. Sci. Data*, 15,
2235–2258, 2023.
- 1148 Hoevers, R., Broothaerts, N., and Verstraeten, G.: The potential of REVEALS-based vegetation
reconstructions using pollen records from alluvial floodplains, *Veg. Hist. Archaeobotany*, 31, 525–540,
2022.
- 1150 Hogg, D.: High-Resolution Analysis of Snow Albedo Interactions in the Arctic, University of Waterloo,
2022.
- 1152 Hollinger, D. Y., Ollinger, S. V., Richardson, A. D., Meyers, T. P., Dail, D. B., Martin, M. E., Scott, N.
A., Arkebauer, T. J., Baldocchi, D. D., and Clark, K. L.: Albedo estimates for land surface models and



- 1154 support for a new paradigm based on foliage nitrogen concentration, *Glob. Change Biol.*, 16, 696–710, 2010.
- 1156 Huybers, P.: Early Pleistocene Glacial Cycles and the Integrated Summer Insolation Forcing, *Science*, 313, 508–511, <https://doi.org/doi:10.1126/science.1125249>, 2006.
- 1158 Iglesias, V. and Whitlock, C.: If the trees burn, is the forest lost? Past dynamics in temperate forests help inform management strategies, *Philos. Trans. R. Soc. B*, 375, 20190115, 2020.
- 1160 Iglesias, V., Whitlock, C., Krause, T. R., and Baker, R. G.: Past vegetation dynamics in the Yellowstone region highlight the vulnerability of mountain systems to climate change, *J. Biogeogr.*, 45, 1768–1780, 2018.
- 1162
- 1164 Ireland, A. W. and Booth, R. K.: Hydroclimatic variability drives episodic expansion of a floating peat mat in a North American kettlehole basin, *Ecology*, 92, 11–18, <https://doi.org/10.1890/10-0770.1>, 2010.
- 1166 Islebe, G. A., Hooghiemstra, H., Brenner, M., Curtis, J. H., and Hodell, D. A.: A Holocene vegetation history from lowland Guatemala, *The Holocene*, 6, 265–271, <https://doi.org/10.1177/095968369600600302>, 1996.
- 1168 Jackson, S. T.: Pollen source area and representation in small lakes of the northeastern United States, *Rev. Palaeobot. Palynol.*, 63, 53–76, 1990.
- 1170 Jackson, S. T. and Lyford, M. E.: Pollen dispersal models in Quaternary plant ecology: assumptions, parameters, and prescriptions, *Bot. Rev.*, 65, 39–75, 1999a.
- 1172 Jackson, S. T. and Lyford, M. E.: Pollen dispersal models in Quaternary plant ecology: Assumptions, parameters, and prescriptions, *Bot. Rev.*, 65, 39–75, 1999b.
- 1174 Jackson, S. T. and Whitehead, D. R.: Holocene vegetation patterns in the Adirondack Mountains, *Ecology*, 72, 641–654, 1991.
- 1176 Jackson, S. T., Overpeck, J. T., Webb, I. T., Keatts, S. E., and Anderson, K. H.: Mapped plant-macrofossil and pollen records of late Quaternary vegetation change in eastern North America, *Quat. Sci. Rev.*, 16, 1–70, 1997.
- 1178
- 1180 Jackson, S. T., Betancourt, J. L., Booth, R. K., and Gray, S. T.: Ecology and the ratchet of events: Climate variability, niche dimensions, and species distributions, *Proc. Natl. Acad. Sci.*, 106, 19685–19692, 2009.
- 1182 Jensen, A. M., Fastovich, D., Watson, B. I., Gill, J. L., Jackson, S. T., Russell, J. M., Bevington, J., Hayes, K., Lininger, K., Rubbelke, C., Schellinger, G. C., and Williams, J. W.: More than one way to kill a spruce forest: The role of fire and climate in the late-glacial termination of spruce woodlands across the southern Great Lakes, *J. Ecol.*, 109, 459–477, <https://doi.org/10.1111/1365-2745.13517>, 2021.
- 1184
- 1186 Kaplan, J. O., Krumhardt, K. M., and Zimmermann, N.: The prehistoric and preindustrial deforestation of Europe, *Quat. Sci. Rev.*, 28, 3016–3034, <https://doi.org/Doi.10.1016/J.Quascirev.2009.09.028>, 2009.
- 1188 Kaplan, J. O., Krumhardt, K. M., Gaillard, M.-J., Sugita, S., Trondman, A.-K., Fyfe, R., Marquer, L., Mazier, F., and Nielsen, A. B.: Constraining the deforestation history of Europe: Evaluation of historical land use scenarios with pollen-based land cover reconstructions, *Land*, 6, 91, 2017.



- 1190 Kaufman, D. S. and Broadman, E.: Revisiting the Holocene global temperature conundrum, *Nature*, 614, 425–435, <https://doi.org/10.1038/s41586-022-05536-w>, 2023.
- 1192 Kelly, R., Chipman, M. L., Higuera, P. E., Stefanova, I., Brubaker, L. B., and Hu, F. S.: Recent burning of boreal forests exceeds fire regime limits of the past 10,000 years, *Proc. Natl. Acad. Sci.*, 110, 13055–13060, <https://doi.org/10.1073/pnas.1305069110>, 2013.
- 1194 Klein Goldewijk, K., Beusen, A., and Janssen, P.: Long-term dynamic modeling of global population and built-up area in a spatially explicit way: HYDE 3.1, *The Holocene*, 20, 565–573, <https://doi.org/10.1177/0959683609356587>, 2010.
- 1196 Klein Goldewijk, K., Beusen, A., van Drecht, G., and de Vos, M.: The HYDE 3.1 spatially explicit database of human-induced global land-use change over the past 12,000 years, *Glob. Ecol. Biogeogr.*, 20, 73–86, <https://doi.org/10.1111/j.1466-8238.2010.00587.x>, 2011.
- 1200 Knight, C. A., Anderson, L., Bunting, M. J., Champagne, M., Clayburn, R. M., Crawford, J. N., Klimaszewski-Patterson, A., Knapp, E. E., Lake, F. K., Mensing, S. A., Wahl, D., Wanket, J., Watts-Tobin, A., Potts, M. D., and Battles, J. J.: Land management explains major trends in forest structure and composition over the last millennium in California’s Klamath Mountains, *Proc. Natl. Acad. Sci.*, 119, e2116264119, <https://doi.org/10.1073/pnas.2116264119>, 2022.
- 1202
- 1204
- 1206 Kuparinen, A., Markkanen, T., Riikonen, H., and Vesala, T.: Modeling air-mediated dispersal of spores, pollen and seeds in forested areas, *Ecol. Model.*, 208, 177–188, 2007.
- 1208 Lacourse, T.: Environmental change controls postglacial forest dynamics through interspecific differences in life-history traits, *Ecology*, 90, 2149–2160, 2009.
- 1210 Lacourse, T. and Adeleye, M. A.: Climate and species traits drive changes in Holocene forest composition along an elevation gradient in Pacific Canada, *Front. Ecol. Evol.*, 10, <https://doi.org/10.3389/fevo.2022.838545>, 2022.
- 1212
- 1214 Lacourse, T., Mathewes, R. W., and Hebda, R. J.: Paleoecological analyses of lake sediments reveal prehistoric human impact on forests at Anthony Island UNESCO World Heritage Site, Queen Charlotte Islands (Haida Gwaii), Canada, *Quat. Res.*, 68, 177–183, <http://dx.doi.org/10.1016/j.yqres.2007.04.005>, 2007.
- 1216
- 1218 Lacourse, T., Delepine, J. M., Hoffman, E. H., and Mathewes, R. W.: A 14,000 year vegetation history of a hypermaritime island on the outer Pacific coast of Canada based on fossil pollen, spores and conifer stomata, *Quat. Res.*, 78, 572–582, <http://dx.doi.org/10.1016/j.yqres.2012.08.008>, 2012.
- 1220 Leopold, E. B. and Boyd, R.: An ecological history of old prairie areas, southwestern Washington, in: *Indians, Fire and the Land*, edited by: Boyd, R., Oregon State University Press, Corvallis OR, 139–166, 1999.
- 1222
- 1224 Lewis, S. L. and Maslin, M. A.: Defining the Anthropocene, *Nature*, 519, 171–180, <https://doi.org/10.1038/nature14258>, 2015.
- 1226 Li, F., Gaillard, M.-J., Cao, X., Herzschuh, U., Sugita, S., Tarasov, P. E., Wagner, M., Xu, Q., Ni, J., and Wang, W.: Towards quantification of Holocene anthropogenic land-cover change in temperate China: A review in the light of pollen-based REVEALS reconstructions of regional plant cover, *Earth-Sci. Rev.*, 203, 103119, 2020.
- 1228



- 1230 Li, F., Gaillard, M.-J., Xie, S., Huang, K., Cui, Q., Fyfe, R., Marquer, L., and Sugita, S.: Evaluation of relative pollen productivities in temperate China for reliable pollen-based quantitative reconstructions of Holocene plant cover, *Front. Plant Sci.*, 14, 2023a.
- 1232 Li, F., Gaillard, M.-J., Cao, X., Herzsuh, U., Sugita, S., Ni, J., Zhao, Y., An, C., Huang, X., Li, Y., Liu, H., Sun, A., and Yao, Y.: Gridded pollen-based Holocene regional plant cover in temperate and northern
1234 subtropical China suitable for climate modelling, *Earth Syst Sci Data*, 15, 95–112, <https://doi.org/10.5194/essd-15-95-2023>, 2023b.
- 1236 Liefert, D. T. and Shuman, B. N.: Pervasive desiccation of North American lakes during the late Quaternary, *Geophys. Res. Lett.*, 47, e2019GL086412, <https://doi.org/10.1029/2019GL086412>, 2020.
- 1238 Lindgren, F., Rue, H., and Lindström, J.: An explicit link between Gaussian fields and Gaussian Markov random fields: the stochastic partial differential equation approach, *J. R. Stat. Soc. Ser. B Stat. Methodol.*, 73, 423–498, 2011.
- 1240
- 1242 Liu, Y., Ogle, K., Lichstein, J. W., and Jackson, S. T.: Estimation of pollen productivity and dispersal: How pollen assemblages in small lakes represent vegetation, *Ecol. Monogr.*, 92, e1513, <https://doi.org/10.1002/ecm.1513>, 2022.
- 1244 Liu, Z., Zhu, J., Rosenthal, Y., Zhang, X., Otto-Bliesner, B. L., Timmermann, A., Smith, R. S., Lohmann, G., Zheng, W., and Elison Timm, O.: The Holocene temperature conundrum, *Proc. Natl. Acad. Sci.*, 111, E3501–E3505, <https://doi.org/10.1073/pnas.1407229111>, 2014.
- 1246
- 1248 Long, C. J., Whitlock, C., Bartlein, P. J., and Millspaugh, S. H.: A 9000-year fire history from the Oregon Coast Range, based on a high-resolution charcoal study, *Can. J. For. Res.*, 28, 774–787, 1998.
- 1250 Long, C. J., Whitlock, C., and Bartlein, P. J.: Holocene vegetation and fire history of the Coast Range, western Oregon, USA, *The Holocene*, 17, 917–926, <https://doi.org/10.1177/0959683607082408>, 2007.
- 1252 Lorant, M. M., Berner, L. T., Goetz, S. J., Jin, Y., and Randerson, J. T.: Vegetation controls on northern high latitude snow-albedo feedback: observations and CMIP 5 model simulations, *Glob. Change Biol.*, 20, 594–606, 2014.
- 1254 MacDonald, G. M.: Postglacial palaeoecology of the subalpine forest-grassland ecotone of southwestern Alberta: new insights on vegetation and climate change in the Canadian Rocky Mountains and adjacent
1256 foothills, *Palaeogeogr. Palaeoclimatol. Palaeoecol.*, 73, 155–173, 1989.
- 1258 MacDonald, G. M. and Cwynar, L. C.: Post-glacial population growth rates of *Pinus contorta* ssp. *latifolia* in western Canada, *J. Ecol.*, 79, 417–429, <https://doi.org/10.2307/2260723>, 1991.
- 1260 Marcott, S. A., Shakun, J. D., Clark, P. U., and Mix, A. C.: A reconstruction of regional and global temperature for the past 11,300 years, *Science*, 339, 1198–1201, 2013.
- 1262 Marlon, J. R., Bartlein, P. J., Gavin, D. G., Long, C. J., Anderson, R. S., Briles, C. E., Brown, K. J., Colombaroli, D., Hallett, D. J., and Power, M. J.: Long-term perspective on wildfires in the western USA, *Proc. Natl. Acad. Sci.*, 109, E535–E543, 2012.
- 1264 Marsicek, J., Shuman, B. N., Bartlein, P. J., Shafer, S. L., and Brewer, S.: Reconciling divergent trends and millennial variations in Holocene temperatures, *Nature*, 554, 92, <https://doi.org/10.1038/nature25464>
1266 <https://www.nature.com/articles/nature25464#supplementary-information>, 2018.



- 1268 McAndrews, J. H. and Turton, C. L.: Canada geese dispersed cultigen pollen grains from prehistoric Iroquoian fields to Crawford Lake, Ontario, Canada, *Palynology*, 31, 9–18, <https://doi.org/10.2113/gspalynol.31.1.9>, 2007.
- 1270 McMichael, C. N. H.: Ecological legacies of past human activities in Amazonian forests, *New Phytol.*, n/a, <https://doi.org/10.1111/nph.16888>, 2020.
- 1272 Mensing, S., Smith, J., Burkle Norman, K., and Allan, M.: Extended drought in the Great Basin of western North America in the last two millennia reconstructed from pollen records, 22nd Pac. Clim. Workshop, 188, 79–89, <https://doi.org/10.1016/j.quaint.2007.06.009>, 2008.
- 1276 Minckley, T. A., Whitlock, C., and Bartlein, P. J.: Vegetation, fire, and climate history of the northwestern Great Basin during the last 14,000 years, *Quat. Sci. Rev.*, 26, 2167–2184, <https://doi.org/10.1016/j.quascirev.2007.04.009>, 2007.
- 1278 Mottl, O., Flantua, S. G. A., Bhatta, K. P., Felde, V. A., Giesecke, T., Goring, S., Grimm, E. C., Haberle, S., Hooghiemstra, H., Ivory, S., Kuneš, P., Wolters, S., Seddon, A. W. R., and Williams, J. W.: Global acceleration in rates of vegetation change over the last 18,000 years, *Science*, 321, 860–864, 2021.
- 1282 Munoz, S. E. and Gajewski, K.: Distinguishing prehistoric human influence on late-Holocene forests in southern Ontario, Canada, *The Holocene*, 20, 967–981, <https://doi.org/10.1177/0959683610362815>, 2010.
- 1284 Munoz, S. E., Schroeder, S., Fike, D. A., and Williams, J. W.: A record of sustained prehistoric and historic land use from the Cahokia region, Illinois, USA, *Geology*, 42, 499–502, <https://doi.org/10.1130/G35541.1>, 2014.
- 1288 Napier, J. D. and Chipman, M. L.: Emerging palaeoecological frameworks for elucidating plant dynamics in response to fire and other disturbance, *Glob. Ecol. Biogeogr.*, n/a, <https://doi.org/10.1111/geb.13416>, 2021.
- 1290 Natural Resources Canada: National Hydro Network, 2022.
- 1292 Nelson, D. M., Hu, F. S., Grimm, E. C., Curry, B. B., and Slate, J. E.: The influence of aridity and fire on Holocene prairie communities in the eastern Prairie Peninsula, *Ecology*, 87, 2523–2536, 2006.
- 1294 Niklas, K. J.: The motion of windborne pollen grains around conifer ovulate cones: implications on wind pollination, *Am. J. Bot.*, 71, 356–374, 1984.
- 1296 Oswald, W. W. and Foster, D. R.: Middle-Holocene dynamics of *Tsuga canadensis* (eastern hemlock) in northern New England, USA, *The Holocene*, 22, 71–78, <https://doi.org/10.1177/0959683611409774>, 2012.
- 1298 Oswald, W. W., Doughty, E. D., Foster, D. R., Shuman, B. N., and Wagner, D. L.: Evaluating the role of insects in the middle-Holocene *Tsuga* decline, *J. Torrey Bot. Soc.*, 144, 35–39, 2017.
- 1300 Oswald, W. W., Foster, D. R., Shuman, B. N., Chilton, E. S., Doucette, D. L., and Duranleau, D. L.: Conservation implications of limited Native American impacts in pre-contact New England, *Nat. Sustain.*, 3, 241–246, <https://doi.org/10.1038/s41893-019-0466-0>, 2020.
- 1302



- 1304 Otto, J., Raddatz, T., and Claussen, M.: Strength of forest-albedo feedback in mid-Holocene climate simulations, *Clim. Past*, 7, 1027–1039, 2011.
- 1306 Paciorek, C. J., Goring, S. J., Thurman, A., Cogbill, C. V., Williams, J. W., Mladenoff, D. J., Peters, J. A.,
1308 Zhu, J., and McLachlan, J. S.: Statistically-estimated tree composition for the northeastern United States at the time of Euro-American settlement, *PLoS One*, 11, e0150087, <http://dx.doi.org/10.1371/journal.pone.0150087>, 2016.
- 1310 Parnell, A. C., Haslett, J., Allen, J. R., Buck, C. E., and Huntley, B.: A flexible approach to assessing synchronicity of past events using Bayesian reconstructions of sedimentation history, *Quat. Sci. Rev.*, 27, 1872–1885, 2008.
- 1312 Payette, S.: A paleo-perspective on ecosystem collapse in boreal North America, edited by: Canadell, J. G. and Jackson, R. B., *Ecosyst. Collapse Clim. Change*, 101–129, https://doi.org/10.1007/978-3-030-71330-0_5, 2021.
- 1316 Payette, S., Filion, L., and Delwaide, A.: Spatially explicit fire-climate history of the boreal forest-tundra (eastern Canada) over the last 2000 years, *Philos. Trans. Biol. Sci.*, 363, 2301–2316, 2008.
- 1318 Payette, S., Couillard, P.-L., Frégeau, M., Laflamme, J., and Lavoie, M.: The velocity of postglacial migration of fire-adapted boreal tree species in eastern North America, *Proc. Natl. Acad. Sci.*, 119, e2210496119, <https://doi.org/10.1073/pnas.2210496119>, 2022.
- 1320 Peros, M. C., Gajewski, K., and Viau, A. E.: Continental-scale tree population response to rapid climate change, competition and disturbance, *Glob. Ecol. Biogeogr.*, 17, 658–669, 2008.
- 1322 Peros, M. C., Munoz, S. E., Gajewski, K., and Viau, A. E.: Prehistoric demography of North America inferred from radiocarbon data, *J. Archaeol. Sci.*, 37, 656–664, 2010.
- 1324 Perrotti, A. G., Ramiadantsoa, T., O’Keefe, J., and Nuñez Otaño, N.: Uncertainty in coprophilous fungal spore concentration estimates, *Front. Ecol. Evol.*, 10, 2022.
- 1326 Pirzamanbein, B., Lindström, J., Poska, A., Sugita, S., Trondman, A.-K., Fyfe, R., Mazier, F., Nielsen, A. B., Kaplan, J. O., Bjune, A., Birks, H. J. B., Giesecke, T., Kangur, M., Latalowa, M., Marquer, L., Smith, B., and Gaillard, M.-J.: Creating spatially continuous maps of past land cover from point estimates: A new statistical approach applied to pollen data, *Ecol. Complex.*, 20, 127–141, <https://doi.org/10.1016/j.ecocom.2014.09.005>, 2014.
- 1330 Pirzamanbein, B., Lindström, J., Poska, A., and Gaillard, M.-J.: Modelling spatial compositional data: Reconstructions of past land cover and uncertainties, *Spat. Stat.*, 24, 14–31, 2018a.
- 1332 Pirzamanbein, B., Lindström, J., Poska, A., and Gaillard, M. J.: Modelling spatial compositional data: Reconstructions of past land cover and uncertainties, *Spat. Stat.*, 24, 14–31, 2018b.
- 1336 Pirzamanbein, B., Poska, A., and Lindström, J.: Bayesian reconstruction of past land cover from pollen data: Model robustness and sensitivity to auxiliary variables, *Earth Space Sci.*, 7, e2018EA00057, 2020.
- 1338 Pongratz, J., Reick, C. H., Raddatz, T., and Claussen, M.: Biogeophysical versus biogeochemical climate response to historical anthropogenic land cover change, *Geophys. Res. Lett.*, 37, L08702, <https://doi.org/10.1029/2010GL043010>, 2010.



- 1340 Prentice, I. C.: Pollen representation, source area, and basin size: toward a unified theory of pollen analysis, *Quat. Res.*, 23, 76–86, 1985.
- 1342 Prentice, I. C., Jolly, D., and BIOME 6000 participants: Mid-Holocene and glacial-maximum vegetation geography of the northern continents and Africa, *J. Biogeogr.*, 27, 507–519, 2000.
- 1344 Prentice, I. C., Harrison, S. P., and Bartlein, P. J.: Global vegetation and terrestrial carbon cycle changes after the last ice age, *New Phytol.*, 189, 988–998, 2011.
- 1346 Rangel, T. F. L. V. B., Diniz-Filho, J. A. F., and Araújo, M. B.: BIOENSEMBLES 1.0, Software for computer intensive ensemble forecasting of species distributions under climate change, 2009.
- 1348 Reimer, P. J., Austin, W. E., Bard, E., Bayliss, A., Blackwell, P. G., Ramsey, C. B., Butzin, M., Cheng, H., Edwards, R. L., and Friedrich, M.: The IntCal20 Northern Hemisphere radiocarbon age calibration curve (0–55 cal kBP), *Radiocarbon*, 62, 725–757, 2020.
- 1350 Richard, P., Fréchette, B., Grondin, P., and Lavoie, M.: Histoire postglaciaire de la végétation de la forêt boréale du Québec et du Labrador, *Nat. Can.*, 144, 63–76, <https://doi.org/10.7202/1070086ar>, 2020.
- 1352 Roberts, N., Fyfe, R. M., Woodbridge, J., Gaillard, M. J., Davis, B. A. S., Kaplan, J. O., Marquer, L., Mazier, F., Nielsen, A. B., Sugita, S., Trondman, A. K., and Leydet, M.: Europe’s lost forests: a pollen-based synthesis for the last 11,000 years, *Sci. Rep.*, 8, 716, <https://doi.org/10.1038/s41598-017-18646-7>, 2018.
- 1356 Rogelj, J., Popp, A., Calvin, K. V., Luderer, G., Emmerling, J., Gernaat, D., Fujimori, S., Strefler, J., Hasegawa, T., Marangoni, G., Krey, V., Kriegler, E., Riahi, K., van Vuuren, D. P., Doelman, J., Drouet, L., Edmonds, J., Fricko, O., Harmsen, M., Havlík, P., Humpenöder, F., Stehfest, E., and Tavoni, M.: Scenarios towards limiting global mean temperature increase below 1.5 °C, *Nat. Clim. Change*, 8, 325–332, <https://doi.org/10.1038/s41558-018-0091-3>, 2018.
- 1360 Roos, C. I.: Scale in the study of Indigenous burning, *Nat. Sustain.*, <https://doi.org/10.1038/s41893-020-0579-5>, 2020.
- 1362 Roos, C. I., Zedeño, M. N., Hollenback, K. L., and Erlick, M. M. H.: Indigenous impacts on North American Great Plains fire regimes of the past millennium, *Proc. Natl. Acad. Sci.*, 115, 8143–8148, <https://doi.org/10.1073/pnas.1805259115>, 2018.
- 1366 Rosenberg, S. M., Walker, I. R., and Mathewes, R. W.: Postglacial spread of hemlock (*Tsuga*) and vegetation history in Mount Revelstoke National Park, British Columbia, Canada, *Can. J. Bot.*, 81, 139–151, 2003.
- 1368 Ruddiman, W. F.: The anthropogenic greenhouse era began thousands of years ago, *Clim. Change*, 61, 261–293, 2003.
- 1370 Ruddiman, W. F.: The Anthropocene, *Annu. Rev. Earth Planet. Sci.*, 41, 4.1–4.24, 2013.
- 1372 Serge, M.-A., Mazier, F., Fyfe, R., Gaillard, M.-J., Klein, T., Lagnoux, A., Galop, D., Githumbi, E., Mindrescu, M., and Nielsen, A. B.: Testing the effect of relative pollen productivity on the REVEALS model: a validated reconstruction of Europe-wide holocene vegetation, *Land*, 12, 986, 2023.



- 1376 Shuman, B., Webb, T., III, Bartlein, P., and Williams, J. W.: The anatomy of a climatic oscillation: vegetation change in eastern North America during the Younger Dryas chronozone, *Quat. Sci. Rev.*, 21, 1777–1791, 2002.
- 1378
- 1380 Shuman, B. N. and Marsicek, J.: The structure of Holocene climate change in mid-latitude North America, *Quat. Sci. Rev.*, 141, 38–51, 2016.
- 1382 Shuman, B. N., Newby, P. C., Huang, Y., and Webb, I., T.: Evidence for the close climatic control of New England vegetation history, *Ecology*, 85, 1297–1310, 2004.
- 1384 Shuman, B. N., Stefanescu, I. C., Grigg, L. D., Foster, D. R., and Oswald, W. W.: A millennial-scale oscillation in latitudinal temperature gradients along the western North Atlantic during the mid-Holocene, *Geophys. Res. Lett.*, 50, e2022GL102556, <https://doi.org/10.1029/2022GL102556>, 2023.
- 1386 Snitker, G., Roos, C. I., Sullivan, A. P., Maezumi, S. Y., Bird, D. W., Coughlan, M. R., Derr, K. M., Gassaway, L., Klimaszewski-Patterson, A., and Loehman, R. A.: A collaborative agenda for archaeology and fire science, *Nat. Ecol. Evol.*, <https://doi.org/10.1038/s41559-022-01759-2>, 2022.
- 1388
- 1390 Spear, R. W., Davis, M. B., and Shane, L. C. K.: Late Quaternary history of low- and mid-elevation vegetation in the White Mountains of New Hampshire, *Ecol. Monogr.*, 64, 85–109, 1994.
- 1392 Stegner, M. A. and Spanbauer, T. L.: North American pollen records provide evidence for macroscale ecological changes in the Anthropocene, *Proc. Natl. Acad. Sci.*, 120, e2306815120, <https://doi.org/10.1073/pnas.2306815120>, 2023.
- 1394 Stephens, L., Fuller, D., Boivin, N., Rick, T., Gauthier, N., Kay, A., Marwick, B., Armstrong, C. G., Barton, C. M., Denham, T., Douglass, K., Driver, J., Janz, L., Roberts, P., Rogers, J. D., Thakar, H., 1396 Altaweel, M., Johnson, A. L., Sampietro Vattuone, M. M., Aldenderfer, M., Archila, S., Artioli, G., Bale, M. T., Beach, T., Borrell, F., Braje, T., Buckland, P. I., Jiménez Cano, N. G., Capriles, J. M., Diez 1398 Castillo, A., Çilingiroğlu, Ç., Negus Cleary, M., Conolly, J., Coutros, P. R., Covey, R. A., Cremaschi, M., Crowther, A., Der, L., di Lernia, S., Doershuk, J. F., Doolittle, W. E., Edwards, K. J., Erlandson, J. M., 1400 Evans, D., Fairbairn, A., Faulkner, P., Feinman, G., Fernandes, R., Fitzpatrick, S. M., Fyfe, R., Garcea, E., Goldstein, S., Goodman, R. C., Dalpoim Guedes, J., Herrmann, J., Hiscock, P., Hommel, P., 1402 Horsburgh, K. A., Hritz, C., Ives, J. W., Junno, A., Kahn, J. G., Kaufman, B., Kearns, C., Kidder, T. R., Lanoë, F., Lawrence, D., Lee, G.-A., Levin, M. J., Lindsoug, H. B., López-Sáez, J. A., Macrae, S., 1404 Marchant, R., Marston, J. M., McClure, S., McCoy, M. D., Miller, A. V., Morrison, M., Motuzaitė Matuzeviciute, G., Müller, J., Nayak, A., Noerwidi, S., Peres, T. M., Peterson, C. E., Proctor, L., Randall, 1406 A. R., Renette, S., Robbins Schug, G., Ryzewski, K., Saini, R., Scheinsohn, V., Schmidt, P., Sebillaud, P., Seitsonen, O., Simpson, I. A., Sołtysiak, A., Speakman, R. J., Spengler, R. N., Steffen, M. L., et al.: 1408 Archaeological assessment reveals Earth’s early transformation through land use, *Science*, 365, 897–902, <https://doi.org/10.1126/science.aax1192>, 2019.
- 1410 Strandberg, G., Kjellström, E., Poska, A., Wagner, S., Gaillard, M. J., Trondman, A. K., Mauri, A., Davis, B. A. S., Kaplan, J. O., Birks, H. J. B., Bjune, A. E., Fyfe, R., Giesecke, T., Kalnina, L., Kangur, M., van 1412 der Knaap, W. O., Kokfelt, U., Kuneš, P., Lata, I owa, M., Marquer, L., Mazier, F., Nielsen, A. B., Smith, B., Seppä, H., and Sugita, S.: Regional climate model simulations for Europe at 6 and 0.2 k BP: 1414 sensitivity to changes in anthropogenic deforestation, *Clim Past*, 10, 661–680, <https://doi.org/10.5194/cp-10-661-2014>, 2014.
- 1416 Strandberg, G., Lindström, J., Poska, A., Zhang, Q., Fyfe, R., Githumbi, E., Kjellström, E., Mazier, F., Nielsen, A. B., Sugita, S., Trondman, A.-K., Woodbridge, J., and Gaillard, M.-J.: Mid-Holocene



- 1418 European climate revisited: New high-resolution regional climate model simulations using pollen-based land-cover, *Quat. Sci. Rev.*, 281, 107431, <https://doi.org/10.1016/j.quascirev.2022.107431>, 2022a.
- 1420 Strandberg, G., Lindström, J., Poska, A., Zhang, Q., Fyfe, R., Githumbi, E., Kjellström, E., Mazier, F.,
1422 Nielsen, A. B., Sugita, S., Trondman, A.-K., Woodbridge, J., and Gaillard, M.-J.: Mid-Holocene European climate revisited: New high-resolution regional climate model simulations using pollen-based land-cover, *Quat. Sci. Rev.*, 281, 107431, <https://doi.org/10.1016/j.quascirev.2022.107431>, 2022b.
- 1424 Sugita, S.: Theory of quantitative reconstruction of vegetation I: pollen from large sites REVEALS regional vegetation composition, *The Holocene*, 17, 229–241, 2007a.
- 1426 Sugita, S.: Theory of quantitative reconstruction of vegetation I: pollen from large sites REVEALS regional vegetation composition., *The Holocene*, 17, 229–241, 2007b.
- 1428 Sugita, S.: Theory of quantitative reconstruction of vegetation II: all you need is LOVE, *The Holocene*, 17, 243–257, 2007c.
- 1430 Sugita, S., Parshall, T., Calcote, R., and Walker, K.: Testing the Landscape Reconstruction Algorithm for spatially explicit reconstruction of vegetation in northern Michigan and Wisconsin, *Quat. Res.*, 74, 289–300, 2010.
- 1432 Sutton, O. G.: 1953: *Micrometeorology*. New York: McGraw-Hill, 1953.
- 1434 TEMPO (Testing Earth System Models with Paleo-Observations): Potential role of vegetation feedback in the climate sensitivity of high-latitude regions: A case study at 6000 years B.P., *Glob. Biogeochem. Cycles*, 10, 727–736, 1996.
- 1436 Theuerkauf, M. and Couwenberg: ROPES reveals past land cover and PPEs From single pollen records, *Front. Earth Sci.*, 6, 2018.
- 1440 Theuerkauf, M., Kuparinen, A., and Joosten, H.: Pollen productivity estimates strongly depend on assumed pollen dispersal, *The Holocene*, DOI: 10.1177/0959683612450194, 2012.
- 1442 Theuerkauf, M., Couwenberg, J., Kuparinen, A., and Liebscher, V.: A matter of dispersal: REVEALSinR introduces state-of-the-art dispersal models to quantitative vegetation reconstruction, *Veg. Hist. Archaeobotany*, 25, 541–553, 2016.
- 1444 Thompson, A. J., Zhu, J., Poulsen, C. J., Tierney, J. E., and Skinner, C. B.: Northern Hemisphere vegetation change drives a Holocene thermal maximum, *Sci. Adv.*, 8, eabj6535, <https://doi.org/10.1126/sciadv.abj6535>, 2022.
- 1446 Thompson, J. R., Carpenter, D. N., Cogbill, C. V., and Foster, D. R.: Four centuries of change in northeastern United States forests, *PLoS One*, 8, e72540, <https://doi.org/10.1371/journal.pone.0072540>, 2013.
- 1450 Thompson, R. S.: Late Quaternary environments in Ruby Valley, Nevada, *Quat. Res.*, 37, 1–15, [https://doi.org/10.1016/0033-5894\(92\)90002-Z](https://doi.org/10.1016/0033-5894(92)90002-Z), 1992.
- 1452 Thompson, R. S., Anderson, K. H., and Bartlein, P. J.: *Atlas of Relations Between Climatic Parameters and Distributions of Important Trees and Shrubs in North America—Introduction and Conifers*, U.S. Department of the Interior, U.S. Geological Survey, 1999.
- 1454



- 1456 Thuiller, W., Lafourcade, B., Engler, R., and Araújo, M. B.: BIOMOD - A platform for ensemble forecasting of species distributions, *Ecography*, 32, 369–373, 2009.
- 1458 Trachsel, M., Dawson, A., Paciorek, C. J., Williams, J. W., McLachlan, J. S., Cogbill, C. V., Foster, D.
1460 R., Goring, S. J., Jackson, S. T., Oswald, W. W., and others: Comparison of settlement-era vegetation reconstructions for STEPPS and REVEALS pollen–vegetation models in the northeastern United States, *Quat. Res.*, 95, 23–42, 2020.
- 1462 Trondman, A.-K., Gaillard, M.-J., Mazier, F., Sugita, S., Fyfe, R., Nielsen, A. B., Twiddle, C., Barratt, P.,
1464 Birks, H. J. B., Bjune, A. E., and others: Pollen-based quantitative reconstructions of Holocene regional vegetation cover (plant-functional types and land-cover types) in Europe suitable for climate modelling, *Glob. Change Biol.*, 21, 676–697, 2015.
- 1466 Trondman, A.-K., Gaillard, M.-J., Sugita, S., Björkman, L., Greisman, A., Hultberg, T., Lagerås, P.,
1468 Lindbladh, M., and Mazier, F.: Are pollen records from small sites appropriate for REVEALS model-based quantitative reconstructions of past regional vegetation? An empirical test in southern Sweden, *Veg. Hist. Archaeobotany*, 25, 131–151, 2016.
- 1470 Umbanhowar, Jr., C. E., Camill, P., Geiss, C. E., and Teed, R.: Asymmetric vegetation responses to mid-Holocene aridity at the prairie-forest ecotone in south-central Minnesota, *Quat. Res.*, 66, 53–66, 2006.
- United States Geological Survey: National Hydrography Dataset (NHD Model v2.3.1), 2022.
- 1472 van Vuuren, D. P., Stehfest, E., Gernaat, D. E. H. J., Doelman, J. C., van den Berg, M., Harmsen, M., de
1474 Boer, H. S., Bouwman, L. F., Daioglou, V., Edelenbosch, O. Y., Girod, B., Kram, T., Lassaletta, L.,
1476 Lucas, P. L., van Meijl, H., Müller, C., van Ruijven, B. J., van der Sluis, S., and Tabeau, A.: Energy, land-use and greenhouse gas emissions trajectories under a green growth paradigm, *Glob. Environ. Change*, 42, 237–250, <https://doi.org/10.1016/j.gloenvcha.2016.05.008>, 2017.
- 1478 Walsh, M. K., Whitlock, C., and Bartlein, P. J.: A 14,300-year-long record of fire–vegetation–climate linkages at Battle Ground Lake, southwestern Washington, *Quat. Res.*, 70, 251–264, <https://doi.org/10.1016/j.yqres.2008.05.002>, 2008.
- 1480 Walsh, M. K., Pearl, C. A., Whitlock, C., Bartlein, P. J., and Worona, M. A.: An 11 000-year-long record
1482 of fire and vegetation history at Beaver Lake, Oregon, central Willamette Valley, *Quat. Sci. Rev.*, 29, 1093–1106, <https://doi.org/10.1016/j.quascirev.2010.02.011>, 2010.
- 1484 Walsh, M. K., Marlon, J. R., Goring, S. J., Brown, K. J., and Gavin, D. G.: A regional perspective on Holocene fire–climate–human interactions in the Pacific Northwest of North America, *Ann. Assoc. Am. Geogr.*, 105, 1135–1157, 2015.
- 1486 Whitlock, C.: Vegetational and climatic history of the Pacific Northwest during the last 20,000 years: Implications for understanding present-day biodiversity, *Northwest Environ. J.*, 8, 5–28, 1992.
- 1488 Whitlock, C., Colombaroli, D., Conedera, M., and Tinner, W.: Land-use history as a guide for forest conservation and management, *Conserv. Biol.*, 32, 84–97, <https://doi.org/10.1111/cobi.12960>, 2018.
- 1490 Whitmore, J., Gajewski, K., Sawada, M., Williams, J., Shuman, B., Bartlein, P., Minckley, T., Viau, A.,
1492 Webb Iii, T., Shafer, S., and others: Modern pollen data from North America and Greenland for multi-scale paleoenvironmental applications, *Quat. Sci. Rev.*, 24, 1828–1848, 2005.



- 1494 Wieczorek, M. and Herzschuh, U.: Compilation of relative pollen productivity (RPP) estimates and taxonomically harmonised RPP datasets for single continents and Northern Hemisphere extratropics, *Earth Syst. Sci. Data*, 12, 3515–3528, 2020.
- 1496 Williams, J. W. and Jackson, S. T.: Novel climates, no-analog communities, and ecological surprises, *Front. Ecol. Environ.*, 5, 475–482, <https://doi.org/10.1890/070037>, 2007.
- 1498 Williams, J. W., Shuman, B. N., and Webb, I., T.: Dissimilarity analyses of late-Quaternary vegetation and climate in eastern North America, *Ecology*, 82, 3346–3362, 2001.
- 1500 Williams, J. W., Shuman, B. N., Webb, T., III, Bartlein, P. J., and Luduc, P. L.: Late-Quaternary vegetation dynamics in North America: scaling from taxa to biomes, *Ecol. Monogr.*, 74, 309–334, 2004.
- 1502 Williams, J. W., Shuman, B., and Bartlein, P. J.: Rapid responses of the Midwestern prairie-forest ecotone to early Holocene aridity, *Glob. Planet. Change*, 66, 195–207, 2009a.
- 1504 Williams, J. W., Shuman, B., and Bartlein, P. J.: Rapid responses of the prairie-forest ecotone to early Holocene aridity in mid-continental North America, *Glob. Planet. Change*, 66, 195–207, 2009b, <https://doi.org/10.1016/j.gloplacha.2008.10.012>.
- 1508 Williams, J. W., Tarasov, P. A., Brewer, S., and Notaro, M.: Late-Quaternary variations in tree cover at the northern forest-tundra ecotone, *J. Geophys. Res. - Biogeosciences*, 116, G01017, doi: 10.1029/2010JG001458, 2011.
- 1510 Williams, J. W., Grimm, E. G., Blois, J., Charles, D. F., Davis, E., Goring, S. J., Graham, R., Smith, A. J., Anderson, M., Arroyo-Cabrales, J., Ashworth, A. C., Betancourt, J. L., Bills, B. W., Booth, R. K., Buckland, P., Curry, B., Giesecke, T., Hausmann, S., Jackson, S. T., Latorre, C., Nichols, J., Purdum, T., Roth, R. E., Stryker, M., and Takahara, H.: The Neotoma Paleoecology Database: A multi-proxy, international community-curated data resource, *Quat. Res.*, 89, 156–177, <https://doi.org/10.1017/qua.2017.105>, 2018.
- 1516 Worona, M. A. and Whitlock, C.: Late Quaternary vegetation and climate history near Little Lake, central Coast Range, Oregon, *Geol. Soc. Am. Bull.*, 107, 867–876, 1995.
- 1518 Zapolska, A., Serge, M. A., Mazier, F., Quiquet, A., Renssen, H., Vrac, M., Fyfe, R., and Roche, D. M.: More than agriculture: Analysing time-cumulative human impact on European land-cover of second half of the Holocene, *Quat. Sci. Rev.*, 314, 108227, <https://doi.org/10.1016/j.quascirev.2023.108227>, 2023.
- 1522